Substituted Pyrazoles as Hepatoselective HMG-CoA Reductase Inhibitors: Discovery of (3*R*,5*R*)-7-[2-(4-Fluoro-phenyl)-4-isopropyl-5-(4-methyl-benzylcarbamoyl)-2*H*-pyrazol-3-yl]-3,5-dihydroxyheptanoic Acid (PF-3052334) as a Candidate for the Treatment of Hypercholesterolemia

Jeffrey A. Pfefferkorn,* Chulho Choi, Scott D. Larsen, Bruce Auerbach, Richard Hutchings, William Park, Valerie Askew, Lisa Dillon, Jeffrey C. Hanselman, Zhiwu Lin, Gina H. Lu, Andrew Robertson, Catherine Sekerke, Melissa S. Harris, Alexander Pavlovsky, Graeme Bainbridge, Nicole Caspers, Mark Kowala, and Bradley D. Tait

Pfizer Global Research and Development, 2800 Plymouth Road, Ann Arbor, Michigan 48105

Received July 12, 2007

In light of accumulating evidence that aggressive LDL-lowering therapy may offer increased protection against coronary heart disease, we undertook the design and synthesis of a novel series of HMG-CoA reductase inhibitors based upon a substituted pyrazole template. Optimizing this series using both structure-based design and molecular property considerations afforded a class of highly efficacious and hepatoselective inhibitors resulting in the identification of (3*R*,5*R*)-7-[2-(4-fluoro-phenyl)-4-isopropyl-5-(4-methyl-benzyl-carbamoyl)-2*H*-pyrazol-3-yl]-3,5-dihydroxy-heptanoic (PF-3052334) as a candidate for the treatment of hypercholesterolemia.

Introduction

Coronary heart disease (CHD)[a] is a leading cause of death, and it represents an increasing burden on healthcare resources worldwide.[1] Epidemiological evidence indicates that hypercholesterolemia is an important risk factor for the CHD;[2] consequently, significant efforts have been undertaken to mitigate this condition. Currently, the most common method of treating hypercholesterolemia is the use of HMG-CoA reductase inhibitors, also known as statins. These drugs block the rate-limiting step of cholesterol biosynthesis, ultimately resulting in up-regulation of the LDL-receptor and the clearing of low density lipoprotein (LDL) particles from the bloodstream.[3] As a class, statins have proven remarkably safe and effective for both primary prevention of coronary heart disease and secondary prevention of coronary events.[4]

Over the past five years, results from several large clinical trials including TNT, MIRACAL, IDEAL, and PROVE-IT have suggested that increasingly aggressive LDL-C lowering therapy may offer further primary and secondary prevention benefits relative to previous, less-aggressive treatment standards.[5] Acknowledging these findings, the National Cholesterol Education Program (NCEP-ATP-III) recently modified its treatment guidelines for patients at risk for CHD. It is now recommended that the highest risk patients achieve a treatment goal of LDL-C < 70 mg/dl, down from the previous treatment goal of 100 mg/dl for this patient group.[6] Moreover, other researchers have suggested that optimal LDL-C levels to prevent atherosclerosis and CHD might be even lower, in the range of 50–70 mg/dl.[7]

Achieving such aggressive LDL-C reductions in patients typically requires the use of high-dose statins alone or in combination with complementary agents, such as the cholesterol absorption inhibitor ezetimibe.[5,8] A potential limitation of high-dose statin therapy is statin-induced myalgia, the muscle pain or weakness that sometimes accompanies statin therapy. While the overall incidence of myalgia is low (2–7% of patients in clinical trials), the likelihood of occurrence increases with drug dose, and it can be a key factor in preventing patient compliance with a treatment regimen.[9a] Physiologically, the mechanism of statin-induced myalgia is complex, but thought to involve, in part, inhibition of HMG-CoA reductase in nonhepatic tissues (particularly muscle), thereby disrupting the biosynthesis of isoprenoid-derived biomolecules important in post-translational protein modification (i.e., prenylation) and electron transport (i.e., ubiquinone).[9]

Fortunately, there is evidence that the likelihood of statin-induced myalgia can be reduced by targeting HMG-CoA reductase inhibitors to hepatic tissues and limiting peripheral exposure.[10] Moreover, it has been demonstrated that the hepatoselectivity of a given HMG-CoA reductase inhibitor is related to its degree of lipophilicity.[10,11] In general, lipophilic statins tend to achieve higher levels of exposure in nonhepatic peripheral tissues, whereas more hydrophilic statins tend to be more hepatoselective. This trend is illustrated experimentally in Table 1, where three benchmark statins spanning a range of lipophilicity were evaluated for their ability to inhibit cholesterol synthesis in both primary rat hepatocyte and rat myocyte (muscle) cells, with the ratio of these two values taken as a measure of hepatoselectivity. As shown and consistent with the earlier findings of others,[12] lipophilic statins such as cerivastatin (which was withdrawn from the market due to high incidences of myalgia and rhabdomyloysis) tend to be nonselective, whereas more hydrophilic statins such as pravastatin and rosuvastatin are hepatoselective. These differences in hepatoselectivity can be rationalized by the fact that lipophilic statins passively and nonselectively diffuse into both hepatocyte and nonhepatocyte cells, while hydrophilic statins (which are

* To whom correspondence should be addressed. Pfizer Global Research and Development, MS 8220-3020, Eastern Point Road, Groton, CT 06340. Phone: 1-860-686-3421. Fax: 1-860-715-4608. E-mail: jeffrey.a.pfefferkorn@pfizer.com.

[a] Abbreviations: CHD, coronary heart disease; HMG-CoA, 3-hydroxy-3-methylglutaryl-CoA; IDEAL, incremental decrease in end points through aggressive lipid-lowering trial; LDL, low density lipoprotein; MIRACAL, myocardial ischemia reduction with acute cholesterol lowering trial; NECP, National Cholesterol Education Program; OATP, organic anion transporting polypeptide; PROVE-IT, pravastatin or atorvastatin evaluation and infection therapy-thrombolysis in myocardial infarction trial; TNT, treating to new targets trial.

10.1021/jm070849r CCC: $40.75
Published on Web 12/12/2007

Table 1. Effect of Inhibitor Lipophilicity on Hepatoselectivity for Selected Known Statins

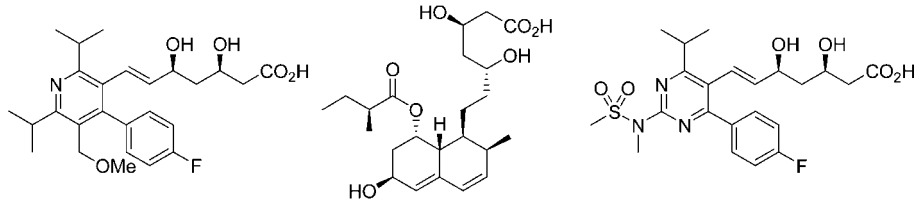

				inhibition of cellular cholesterol synthesis[b]		
cmpd	LogP[a] (pH 7.4)	cLogD (pH 7.4)	HMG-CoA[b] IC_{50} (nM)	hepatocyte IC_{50} (nM)	myocyte IC_{50} (nM)	myocycte/hepatocyte ratio
cerivastatin	1.66	1.76	2.8 ± 0.5	1.7 ± 0.2	3.0 ± 0.3	1.8
pravastatin	−0.67	0.70	13 ± 1	17 ± 2	7600 ± 3200	450
rosuvastatin	NA[c]	−2.63	3.1 ± 0.2	0.3 ± 0.1	250 ± 20	830

[a] See ref 11d. [b] Assay values reported as the mean ± SEM of $n \geq 2$ independent determinations. [c] NA = not available.

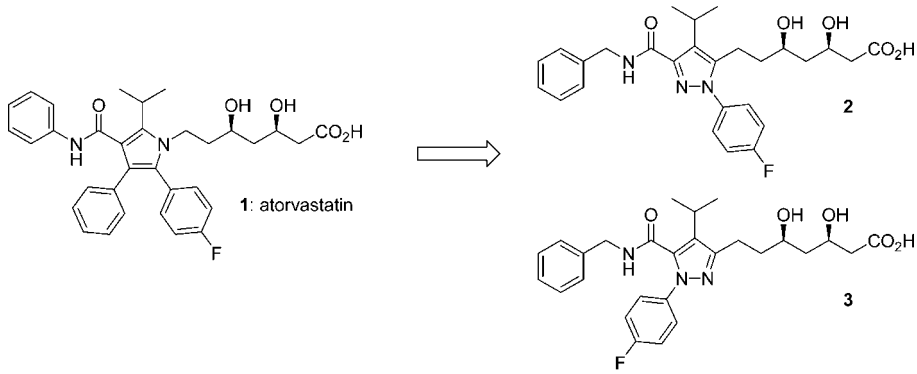

Figure 1. Structures of atorvastatin (**1**) and pyrazole-based HMG-CoA reductase inhibitors **2** and **3**.

inherently less membrane-permeable) rely to a greater extent on active transport into hepatocyte cells to exert their effects.[10,13] Pravastatin and rosuvastatin, among other statins, have been shown to be substrates for active transport via members of the organic anion transporting polypeptide (OATP) family of membrane transporters, which are principally expressed in hepatocytes.[10c,13–15]

One potential limitation of achieving high hepatoselectivity via reduced inhibitor lipophilicity, however, is that as a compound becomes more hydrophilic and, therefore, less permeable, its oral absorption is typically impeded (provided that no compensating transport mechanism is present in the gastrointestinal system); consequently, achieving the appropriate level of inhibitor lipophilicity is pivotal to balancing selectivity and efficacy.

To meet the challenge of finding novel HMG-CoA reductase inhibitors with the efficacy and tolerability profiles needed to help patients achieve aggressive LDL reduction goals, we undertook a discovery effort to identify a novel class of inhibitors with best-in-class preclinical efficacy and hepatoselectivity. We strategically envisioned meeting this objective through modification of the atorvastatin (**1**) template. Specifically, we sought to replace the pyrrole core of atorvastatin with alternative five-membered heterocycles of lower inherent lipophilicity and/or substitution.[16] Of particular interest was a pyrazole core system, as exemplified by isomeric prototypes **2** and **3** (Figure 1). Synthesis of **2** and **3** (vida infra), followed by evaluation against HMG-CoA reductase, revealed that pyrazole **2** (IC_{50} = 4.7 nM) had activity comparable to the parent atorvastatin (IC_{50} = 12 nM) whereas regioisomer **3** (IC_{50} = 520 nM) was substantially less active. We subsequently undertook structure–activity studies on **2**, focusing on modification of the amide motif, to optimize its hepatoselectivity and in vivo efficacy.

Chemistry

Substituted pyrazole analogs for the current studies were synthesized as outlined in Schemes 1–4. Initial efforts focused on construction of a heterocyclic core, which could be utilized as a versatile intermediate for subsequent analog synthesis. As shown in Scheme 1, 4-fluoroaniline (**4**) was first converted to its corresponding diazonium salt by treatment with $NaNO_2$/HCl, and this intermediate was reacted with methyl 2-chloroacetoacetate to give hydrazonoyl chloride **5**.[17] Treatment of **5** with Ag_2CO_3 resulted in in situ generation of nitrilimine **6**, which was engaged in a stereoselective 1,3-dipolar cycloaddition with *E*-enone **8** as the dipolarophile to provide a 5:1 mixture of regioisomeric dihydropyrazoles, with **9** as the major regioisomer.[17,18] The regiochemistry of **9** was confirmed upon ceric ammonium nitrate oxidation to pyrazole **10**, a crystalline solid that was subjected to small molecule X-ray analysis, as shown in Scheme 1.

With pyrazole **10** in hand, inhibitor **2** was completed, as outlined in Scheme 2. The benzyl ester of **10** was first converted to the carboxaldehyde of **11** using a three-step sequence that included (a) hydrogenolysis to a carboxylic acid; (b) reduction to the corresponding alcohol with BH_3·THF;[19] and (c) oxidation to an aldehyde with Dess−Martin periodinate. The methyl ester of **11** was saponified with aqueous NaOH to provide carboxylic acid **12**, which was engaged in an EDCI-mediated coupling with benzyl amine to provide amide **13**. Attachment of the 3,5-dihydroxyhexanoic acid side chain onto the pyrazole core was anticipated to be accomplished via a Wittig olefination reaction that first required conversion of **13** into an appropriate ylide precursor.[20] Hence, the carboxaldehyde of **13** was reduced to

Scheme 1. Synthesis and X-ray Structure of Pyrazole Intermediate **10**[a]

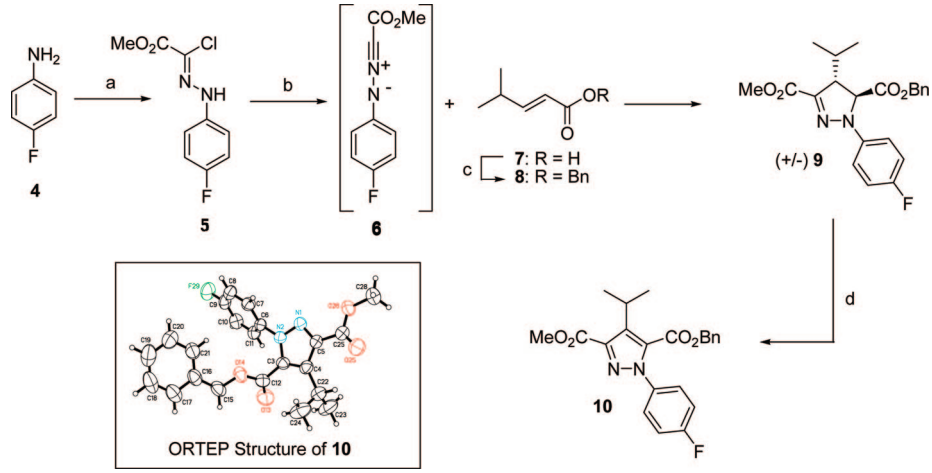

[a] Reagents and conditions: (a) (i) $NaNO_2$, HCl, MeOH, 0 °C, 0.25 h; (ii) methyl-2-chloroacetoacetate, MeOH, 25 °C, 12 h, 94%; (b) Ag_2CO_3, dioxane, 25 °C, 48 h, 73%; (c) BnBr, K_2CO_3, acetone, 56 °C, 16 h, 98%; (d) ceric ammonium nitrate, THF/H_2O, 0 °C, 1 h, 65%.

the corresponding alcohol and then treated with $Ph_3P \cdot HBr$ at elevated temperature to afford phosphonium salt **14** in excellent yield. In parallel, Swern oxidation of commercially available alcohol **15** provided aldehyde **16** as a suitable coupling partner.[21] In the olefination event, phosphonium salt **14** was deprotonated with LiHMDS at low temperature, and a solution of aldehyde **16** was added to provide olefin **17** in moderate yield as an inconsequential mixture of cis/trans isomers. Treatment of **17** with HCl/MeOH effected cleavage of the acetonide protecting group, and the side chain olefin was then hydrogenated over 10% Pd/C to afford **18**. Finally, the terminal ester of **18** was saponified with aqueous NaOH to provide compound **2** as a carboxylate sodium salt.

Scheme 3 illustrates the synthesis of inhibitor **3**, a regioisomer of inhibitor **2**, utilizing minor modifications to the synthetic route previously described. Hydrogenolysis of the benzyl ester of **10** provided the corresponding carboxylic acid **19**, which was subjected to an EDCI-mediated coupling with benzyl amine to give benzyl amide **20**. The methyl ester of **20** was then saponified, and the resulting carboxylic acid reduced with $BH_3 \cdot THF$ to afford alcohol **22**. Treatment of **22** with PBr_3 converted this alcohol to an alkyl bromide that was then reacted with Ph_3P at elevated temperature, resulting in the formation of phosphonium salt **23** in good yield. Notably, this two-step conversion of **22**→**23** was found to be more efficient than the single-step sequence previously described for **13**→**14** (Scheme 2) owing to the extended reaction time required for this later transformation. Finally, using the same four-step sequence (Wittig reaction, acetonide deprotection, hydrogenation, and saponification) described above, phosphonium salt **23** was converted to **3**, which was isolated as its carboxylate sodium salt.

While the synthetic routes described in Schemes 2 and 3 provided facile assess to many of the analogs described herein, a second route, employing an alternative method of side chain attachment, was also utilized for the synthesis of selected analogs. This alternative route is outlined in Scheme 4 for the synthesis of inhibitor **32**. As shown, amide **26** was prepared as previously described and engaged in a Wittig olefination reaction with stabilized ylide **27** (prepared according to the method of Konoike[22]) to provide *E*-olefin **28** in good overall yield. The TBS-protected side chain hydroxyl of **28** was then liberated by treatment with aqueous HF to provide β-hydroxy ketone **29**, which was subjected to a stereoselective *syn*-reduction with Et_2BOMe and $NaBH_4$ to produce *syn*-diol **30**.[23] Finally, the synthesis was completed by hydrogenation of the side chain olefin followed by saponification of the terminal ester to provide inhibitor **32** as its carboxylate sodium salt.

The synthetic routes outlined in Schemes 14 were subsequently utilized for the preparation of all analogs in these studies.

Results and Discussion

Structure–Activity Studies. Our SAR studies in this pyrazole series focused on optimizing potency, hepatoselectivity, and in vivo efficacy; importantly and as discussed below, achieving the necessary balance between these parameters required manipulation of analog structure and lipophilicity. All new analogs were first evaluated in an HMG-CoA reductase enzyme inhibition assay. Additionally, the ability of analogs to block cholesterol synthesis in both rat hepatocyte and myocyte cell lines was evaluated; moreover, comparison of these two values was utilized as a measurement of hepatoselectivity. As a guideline, inhibitors with potent hepatocyte activity (hepatocyte $IC_{50} < 10$ nM) and good hepatoselectivity (myocyte/hepatocyte ratio preferably >1000) were selected for further evaluation in both acute and chronic animal efficacy models. Our acute model, performed in hamsters, measured a compound's ability to inhibit cholesterol synthesis. To get a preliminary assessment of a compound's duration of action, two time points were measured in separate animal groups. In one group (denoted as $t = 2$–4 h group), animals were dosed with drug (10 mpk) at $t = 0$ h then given an intraperitoneal injection of ^{14}C sodium acetate at $t = 2$ h, and finally, blood samples were obtained at $t = 4$ h and analyzed for ^{14}C cholesterol levels, which were compared to untreated control animals to determine percent inhibition of acute cholesterol synthesis. In a second group (denoted as $t = 4$–6 h group), animals were again dosed with drug (10 mpk) at $t = 0$ h then given an intraperitoneal injection of ^{14}C sodium acetate at $t = 4$ h, and finally, blood samples were obtained at $t = 6$ h and analyzed for ^{14}C cholesterol levels, which were compared to untreated control animals. Comparison of the results from these two assays afforded a preliminary measure of a compound's duration of action, which was utilized for prioritizing compounds for further evaluation. Based upon these acute efficacy data, compounds of interest were then selected for evaluation in a chronic (7 day) LDL lowering study that was performed in chow-fed guinea pigs. This chronic study was initially performed at a single dose of drug (10 or 20 mpk),

Scheme 2. Synthesis of Pyrazole Prototype Analog **2**[a]

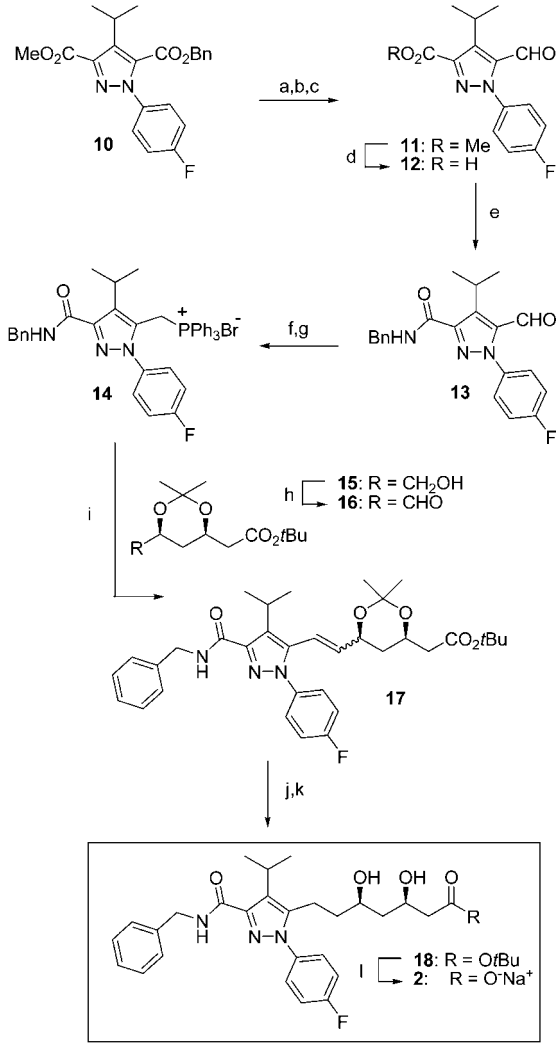

[a] Reagents and conditions: (a) H_2, 10% Pd/C, MeOH, 25 °C, 3 h, 99%; (b) BH_3·THF, THF, 65 °C, 3.5 h, 90%; (c) Dess−Martin periodinate, $NaHCO_3$, CH_2Cl_2, 25 °C, 4 h, 84%; (d) NaOH (aq), MeOH, 60 °C, 4 h, 79%; (e) $BnNH_2$, EDCI, HOBt·H_2O, CH_2Cl_2, 25 °C, 4 h, 39%; (f) $NaBH_4$, THF/MeOH, 0 °C, 0.5 h, 87%; (g) Ph_3P·HBr, MeCN, 80 °C, 48 h, 98%; (h) see ref *21*; (i) **16**, LiHMDS, THF, −78 °C, 5.5 h, 50%; (j) HCl (aq), MeOH, 25 °C, 3 h, 69%; (k) H_2, 10% Pd/C, MeOH, 25 °C, 3 h, 59%; (l) NaOH (aq), MeOH, 25 °C, 48 h, 94%.

Scheme 3. Synthesis of Pyrazole Prototype Analog **3**[a]

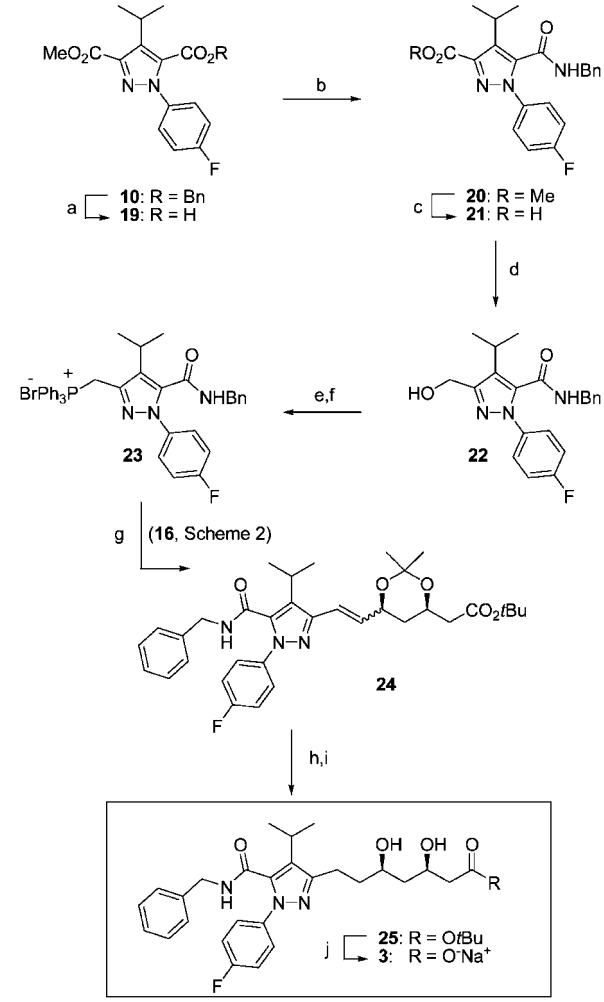

[a] Reagents and conditions: (a) H_2, 10% Pd/C, MeOH, 25 °C, 3 h, 99%; (b) $BnNH_2$, EDCI, HOBt·H_2O, CH_2Cl_2, 25 °C, 8 h, 57%; (c) NaOH (aq), MeOH, 60 °C, 3 h, 98%; (d) BH_3·THF, THF, 65 °C, 4 h, 35%; (e) PBr_3, CH_2Cl_2, 25 °C, 12 h, 100%; (f) Ph_3P, 80 °C, 14 h, 100%; (g) **16**, LiHMDS, THF, −78 °C, 2.5 h, 63%; (h) HCl (aq), MeOH, 25 °C, 1.5 h, 93%; (i) H_2, 10% Pd/C, MeOH, 25 °C, 4 h, 56%; (j) NaOH (aq), MeOH, 25 °C, 16 h, 97%.

results were compared against the benchmark compound rosuvastatin, and analogs with comparable activity were then evaluated in full dose response studies.

As shown in Table 2, preliminary SAR efforts focused on evaluating substituted secondary benzyl amides. Because the prototype compound **2**, which contained an unsubstituted benzyl amide, lacked sufficient hepatoselectivity (myocyte IC_{50}/hepatocyte IC_{50} < 1000) substituents were added to reduce lipophilicity and, consequently, improve selectivity. As illustrated, compounds **35**–**38** demonstrated sufficient hepatoselectivity to warrant acute in vivo evaluation. Preliminary acute in vivo evaluation was done at the $t = 6$ h time point with actives (defined as −10% or greater inhibition) then also evaluated at the $t = 4$ h time point. As shown, analogs **35** and **36** both exhibited good acute efficacy, whereas the more hydrophilic compounds **37** and **38** were not acutely efficacious. Interestingly, inspection of the analogs of Table 2 confirmed that, within this limited series, hepatoselectivity generally increased as lipophilicity decreased (with the exception of **35**); additionally, acute in vivo efficacy tended to also diminish as inhibitor lipophilicity decreased (particularly for **37** and **38**), presumably as a result of reduced oral absorption.

A second type of amide modification explored was *N*-alkylation, as highlighted in Table 3. Comparison of secondary amide **2** to its *N*-methylated tertiary amide counterpart **39** revealed that the two compounds had similar potency in hepatocyctes [IC_{50} = 0.3 nM (**2**) vs 0.2 nM (**39**)], but interestingly, the *N*-methyl derivative **39** was 30-fold less active against myocytes [IC_{50} = 100 nM (**2**) vs 3100 nM (**39**)]. In addition to its increased hepatoselectivity, *N*-methyl amide **39** also exhibited good acute in vivo efficacy, as illustrated in Table 3. Increasing the size of the *N*-alkyl group to ethyl (**40**) and *i*-propyl (**41**) resulted in decreased potency for inhibition of hepatocyte cholesterol synthesis.

To further capitalize on the selectivity and efficacy observed for compound **39**, we next sought to investigate the effect of further substitution on this analog, as shown in Table 4, where a series of alkyl, alkoxy, and fluoro groups were installed at the ortho, meta, and para position of the benzyl ring. In nearly all cases, these compounds had excellent potency and selectivity; however, optimal acute in vivo efficacy was observed for

Scheme 4. Alternative Method for the Synthesis of Pyrazole Analogs Illustrated for Compound **32**[a]

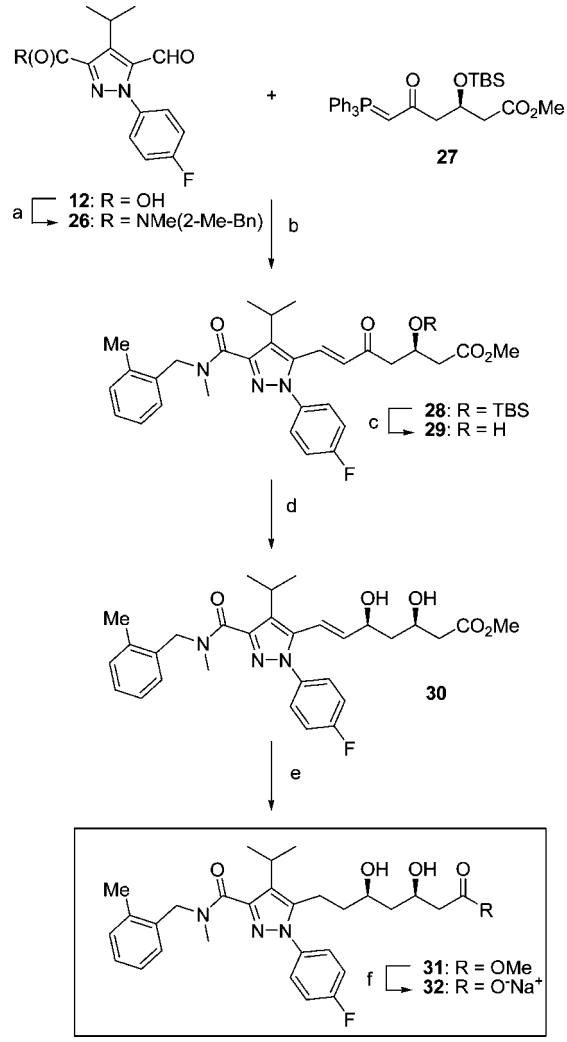

[a] Reagents and conditions: (a) (2-Me)-PhCH$_2$N(Me)H, EDCI, HOBt·H$_2$O, CH$_2$Cl$_2$, 25 °C, 6 h, 72%; (b) toluene, 95 °C, 16 h, 98%; (c) HF (48% aq), MeCN, 25 °C, 16 h, 98%; (d) Et$_2$BOMe, NaBH$_4$, THF/MeOH, −78 °C, 3 h, 81%; (e) H$_2$, 10% Pd/C, MeOH, 25 °C, 4 h, 66%; (f) NaOH (aq), MeOH, 25 °C, 12 h, 99%.

compounds **48** and **49** bearing 2,4-F and a 2,3-F substituent patterns, respectively.

A final type of analog modification focused on the benzylic position of benzyl amide **37**, as illustrated in Table 5. Specifically, we sought to understand the effect of α-methylation of the benzyl amide, as illustrated by stereosiomers **50** and **51**. While **50** demonstrated superior activity relative to its diastereomeric counterpart **51**, its selectivity and efficacy were similar to the unsubstituted case **39**; however, structural biology studies of **50** revealed an interesting observation.

Figure 2 shows an X-ray structure of compound **50** bound to the active site of HMG-CoA reductase.[24] While the compound binds in a mode consistent with other known HMG-CoA reductase inhibitors,[25] inspection of the relative positions of the *N*-methyl and α-methyl groups reveal that (in the inhibitor's bound conformation) these two groups experience a steric interaction that is intermediate between gauche and eclipsing. This observation suggested that the bound configuration of **50** was not a low energy conformation. Moreover, it appeared that the two alkyl groups might be conveniently tethered into a ring to restrict the amide motif into its active conformation. To evaluate this hypothesis, racemic 2-phenyl pyrrolidine, 2-phenyl piperidine, and 3-phenyl piperidine were utilized to prepare **52**, **53**, and **54**, respectively, as 1:1 diastereomeric mixtures. Among these compounds, **54** provided the best combination of potency, selectivity, and efficacy. Subsequently, the two individual stereoisomers of **54** were independently prepared and assayed, resulting in the identification of **55** as the more active component. Encouragingly, this compound had outstanding acute efficacy; unfortunately, the selectivity of **55** against the myocycte cell line was somewhat diminished.

Chronic Efficacy Studies To Enable Candidate Selection. In an effort to better evaluate the therapeutic potential of this series of HMG-CoA reductase inhibitors, analogs demonstrating good selectivity and acute efficacy were selected for chronic in vivo characterization. Specifically, these compounds were evaluated for their ability to lower LDL cholesterol in a chow-fed guinea pigs over a 7 day period with daily oral administration of drug at a single dose (10 or 20 mpk). Efficacy of the new analogs was benchmarked against rosuvastatin, and compounds with comparable single-dose efficacy were selected for dose−response studies. As shown in Table 6, analogs **35**, **36**, and **49** demonstrated chronic efficacy comparable to rosuvastatin at the dose evaluated, while the remaining compounds were less active. As a result of these single dose data **35**, **36**, and **49** were then evaluated in dose−response studies.

During the dose−response studies of these three compounds, compound **36** was found to have inferior efficacy relative to the benchmark rosuvastatin (data not shown) and was therefore discarded. By contrast, both **35** and **49** demonstrated efficacy comparable to if not better than rosuvastatin. Unfortunately, difficulties obtaining a suitable crystal form of inhibitor **49** prevented further development of this compound. Encouragingly, as shown in Figure 3, comparison of the dose response of **35** (represented as PF-3052334) versus that of rosuvastatin and pravastatin revealed that with an $ED_{50} = 3.6$ mpk it was approximately 3 times more efficacious than rosuvastatin ($ED_{50} = 9.3$ mpk) and 27 times more efficacious than pravastatin ($ED_{50} = 100$ mpk) in this animal model. Considering both the good hepatoselectivity (>800-fold) and the excellent LDL-lowering efficacy of **35**, this compound was advanced forward as a candidate that is currently under evaluation in a phase I trial, the results of which will be reported separately.

Retrospective Analysis of Lipophilicity and Selectivity. As described at the outset, a key element of our current strategy was to understand the relationship between inhibitor lipophilicity and hepatoselectivity and to use the former as a prediction of the latter to enable efficient analog design and prioritization. During the course of our studies, we generated a cohort of pyrazole analogs that spanned a range of lipophilicity (cLogD = −0.01 to −2.25) but still maintained relatively similar inherent potencies for inhibition of the HMG-CoA enzyme reductase enzyme. Furthermore, for each compound, we had a hepatoselectivity ratio based upon comparison of hepatocyte and myocyte inhibition values. With this data in hand, we were positioned to undertake a retrospective analysis on the series to determine whether or not cLogD was predictive of hepatoselectivity for analogs in this series. This analysis is presented graphically in Figure 4 where a subset of analogs with HMG-CoA $IC_{50} = 1$–10 nM[26] was utilized to generate plots of cLogD versus log (myocyte IC_{50}) [A], log (hepatocyte IC_{50}) [B], and log (myocyte/hepatocyte) [C]. Several correlations were noted and exemplified with trend lines on the plots. First, as exemplified in Plot [A], myocyte potency decreased with increasing inhibitor hydrophilicity (i.e., lower cLogD). This is consistent with the fact that membrane permeability typically decreases

Table 2. Structure and Biological Activity of Tertiary Amide Analogs 33–38

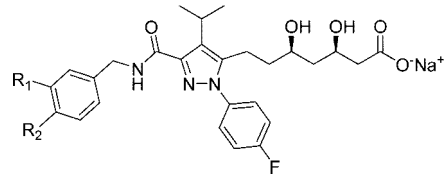

				inhibition of cellular cholesterol synthesis[a]		inhibition of in vivo cholesterol synthesis[b]		
cmpd	R_1	R_2	HMG-CoA[a] IC_{50} (nM)	hepatocyte IC_{50} (nM)	myocyte IC_{50} (nM)	t = 2–4 h (10 mpk)	t = 4–6 h (10 mpk)	cLogD (pH 7.4)
rosuvastatin			3.1 ± 0.2	0.3 ± 0.1	250 ± 20	−76%	−46%	−2.63
2	H	H	4.7 ± 1.0	0.3 ± 0.1	100 ± 10			−0.47
33	H	OMe	2.8[c]	0.4[c]	460[c]			−0.56
34	H	F	3.8 ± 0.5	0.7[c]	490 ± 40			−0.42
35	H	Me	1.9 ± 1.1	0.9 ± 0.1	730 ± 20	−74%	−15%	−0.01
36	CH_2OMe	H	7.0 ± 1.4	0.7 ± 0.1	1800 ± 800	−71%	−19%	−0.73
37	CN	H	2.2 ± 1.0	1.4 ± 0.3	2400[c]		NA[d]	−1.04
38	H	C (O) NMe_2	25[c]	23[c]	21000[c]		NA	−2.25

[a] Assay values reported as the mean ± SEM of $n \geq 2$ independent determinations unless otherwise noted. [b] Data represent the mean of the percent change from the control group (n = 8/group). Interanimal variability in ^{14}C cholesterol levels was typically <20%. [c] Data from n = 1 determination. [d] NA = not active.

Table 3. Structure and Biological Activity of Tertiary Amide Analogs 39–41

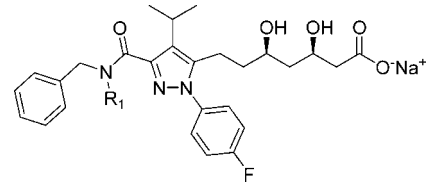

			inhibition of cellular cholesterol synthesis[a]		inhibition of in vivo cholesterol synthesis[b]		
cmpd	R_1	HMG-CoA[a] IC_{50} (nM)	hepatocyte IC_{50} (nM)	myocyte IC_{50} (nM)	t = 2–4 h (10 mpk)	t = 4–6 h (10 mpk)	cLogD (pH 7.4)
rosuvastatin		3.1 ± 0.2	0.3 ± 0.1	250 ± 20	−76%	−43%	−2.63
2	H	4.7 ± 1.0	0.3 ± 0.1	100 ± 10			−0.47
39	Me	5.9 ± 1.2	0.2 ± 0.1	3100 ± 500	−61%	−16%	−1.20
40	Et	3.8 ± 0.9	5.5 ± 0.8	4400 ± 500		NA[d]	−0.67
41	*i*Pr	9.8[c]	10 ± 2	9800[c]			−0.32

[a] Assay values reported as the mean ± SEM of $n \geq 2$ independent determinations, unless otherwise noted. [b] Data represent the mean of the percent change from the control group (n = 8/group). Interanimal variability in ^{14}C cholesterol levels was typically <20%. [c] Data from n = 1 determination. [d] NA = not active.

as inhibitor hydrophilicity increases; therefore, if these inhibitors penetrate the myocytes via passive diffusion (as anticipated), one would expect the correlation that was observed.[27] By contrast, examination of Plot [B] reveals that hepatocyte potency was somewhat independent of inhibitor lipophilicity. In fact, there was a slight trend suggesting that cellular potency in hepatocytes actually increased as inhibitor hydrophilicity increased. This is counter to a passive diffusion model and suggests that these inhibitors are likely experiencing active transport into the hepatocyte cells. Lastly, the utility of cLogD as a tool for predicting hepatoselectivity in the current series is evaluated in Plot [C]. As shown, a modest correlation exits (R^2 = 0.6) between cLogD and the hepatoselectivity (defined as myocyte/hepatocyte activity) such that predicted lipophilicity might serve as a tool for prioritizing future analogs.

Conclusion

In response to the need for increasingly effective yet well-tolerated HMG-CoA reductase inhibitors, we have described herein the synthesis and evaluation of a series of hepatoselective and highly efficacious pyrazole-based inhibitors. These efforts resulted in the identification of **35** as a candidate for the treatment of hypercholesterolemia. Finally, through a retrospective analysis, we demonstrated the utility of calculated lipophilicity as a design tool for predicting the hepatoselectivity of analogs in this series.

Experimental Section

General. All reagents and solvents were used as received from commercial sources unless otherwise noted. Alcohol **15** was purchased from Kanaka Corporation and converted to aldehyde **16**, as previously described.[21] [3-^{14}C]-HMG-CoA (57.0 mCi/mmol) was purchased from Amersham Biosciences, U.K. HMG-CoA, mevalonolactone, beta-NADPH (beta-nicotinamide adenine dinucleotide phosphate, reduced form) were purchased from Sigma Chemical Co. AG 1–8× resin was purchased from Bio-Rad Laboratory.

All experiments were conducted under an inert nitrogen atmosphere unless otherwise noted. ^1H NMR spectra were recorded on a Varian 400 MHz Nuclear Magnetic Resonance Spectrometer. ^1H NMR spectra were recorded in $CDCl_3$, CD_3OD, or d_6-DMSO, and chemical shifts are reported relative to the residual solvent peak. The following abbreviations were used to assign spectra: s = singlet, d = doublet, t = triplet, q = quartet, s = septet, m = multiplet. Mass spectral analysis was conducted on a Waters Micromass ZQ instrument. HPLC analysis was conducted according to method A, B, or C, with the retention time (t_R) expressed in min at UV detection of 254 nM. HPLC method A: Agilent 1100 HPLC with chromatography performed on a Zorbax Eclipse XBD-C_8 column (4.6 × 150 mm, 5 μm) at 25 °C. The mobile phase was a 15 min binary gradient of acetonitrile (containing 0.1% TFA) and water (20–90%). HPLC method B: Agilent HPLC with chromatography

Table 4. Structure and Biological Activity of Substituted Tertiary Amide Analogs 32, 39, and 42–49

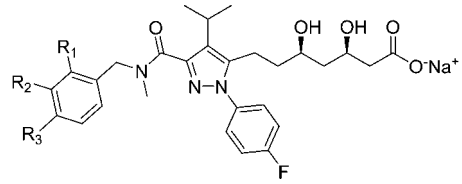

					inhibition of cellular cholesterol synthesis[a]		inhibition of in vivo cholesterol synthesis[b]		
cmpd	R_1	R_2	R_3	HMG-CoA[a] IC_{50} (nM)	hepatocyte IC_{50} (nM)	myocyte IC_{50} (nM)	t = 2–4 h (10 mpk)	t = 4–6 h (10 mpk)	cLogD (pH 7.4)
rosuvastatin				3.1 ± 0.2	0.3 ± 0.1	250 ± 20	−76%	−46%	−2.63
39	H	H	H	5.9 ± 0.1	0.2 ± 0.1	3100 ± 500	−61%	−16%	−1.20
32	Me	H	H	16[c]	2.1[c]	2600[c]		−18%	−0.74
42	H	Me	H	6.1[c]	0.6 ± 0.1	4800 ± 2400	−72%		−0.74
43	H	H	Me	9.9[c]	1.8[c]	4000[c]			−0.74
44	H	H	OMe	12 ± 2	0.3 ± 0.1	5800[c]	−57%		−1.29
45	F	H	H	4.8 ± 2.3	0.5 ± 0.2	17000 ± 8000	−69%	−30%	−1.15
46	H	F	H	3.9 ± 0.9	0.2 ± 0.1	6000 ± 300	−65%	NA[d]	−1.15
47	H	H	F	6.6 ± 1.0	0.5 ± 0.1	6000[c]	−71%	NA	−1.15
48	F	H	F	7.0 ± 0.7	2.1 ± 0.7	4400 ± 2400	−82%	−17%	−1.06
49	F	F	H	9.0 ± 2.7	0.6 ± 0.1	5700 ± 1300	−81%	−22%	−1.06

[a] Assay values reported as the mean ± SEM of $n \geq 2$ independent determinations, unless otherwise noted. [b] Data represent the mean of the percent change from the control group (n = 8/group). Interanimal variability in ^{14}C cholesterol levels was typically <20%. [c] Data from n = 1 determination. [d] NA = not active.

Table 5. Structure and Biological Activity of Analogs 39 and 50–55

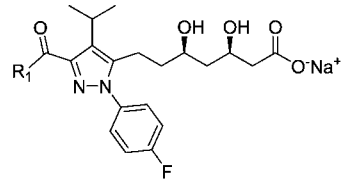

Compound	R_1	HMG-CoA[a] IC_{50} (nM)	*Inhibition of cellular cholesterol synthesis*[a]		*Inhibition of in vivo cholesterol synthesis*[b]		cLogD (pH 7.4)
			Hepatocyte IC_{50} (nM)	Myocyte IC_{50} (nM)	t = 2 - 4h (10 mpk)	t = 4 - 6h (10 mpk)	
Rosuvastatin		3.1 ± 0.2	0.3 ± 0.1	250 ± 20	-76%	-46%	-2.63
39		5.9 ± 1.2	0.2 ± 0.1	3100 ± 500	-61%	-16%	-1.20
50		1.5 ± 0.2	0.3 ± 0.1	1900 ± 400	-62%	-10%	-0.86
51		45[c]	3.5[c]	41000[c]	-	-	-0.86
52		7.3[c]	4.0[c]	130[c]	-	-	-0.97
53		6.1[c]	1.1[c]	330[c]	-	-	-0.41
54	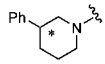	1.5[c]	0.4[c]	680[c]	-80%	-15%	-0.42
55	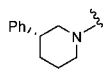	2.0 ± 0.1	0.3 ± 0.1	310 ± 60	-78%	-	-0.42

[a] Assay values reported as the mean ± SEM of $n \geq 2$ independent determinations, unless otherwise noted. [b] Data represent the mean of the percent change from the control group (n = 8/group). Interanimal variability in ^{14}C cholesterol levels was typically <20%. [c] Data from n = 1 determination.

performed on a Phenomenex Develosil Combi-RP C30 140A column (4.6 × 50 mm, 3 μm) at 45 °C. The mobile phase was a 4.5 min binary gradient of acetonitrile (containing 0.1% HCO_2H) and water (2–50%). HPLC method C: Agilent HPLC with chromatography performed on a Phenomenex Develosil Combi-RP C30 140A column (4.6 × 50 mm, 3 μm) at 45 °C. The mobile phase

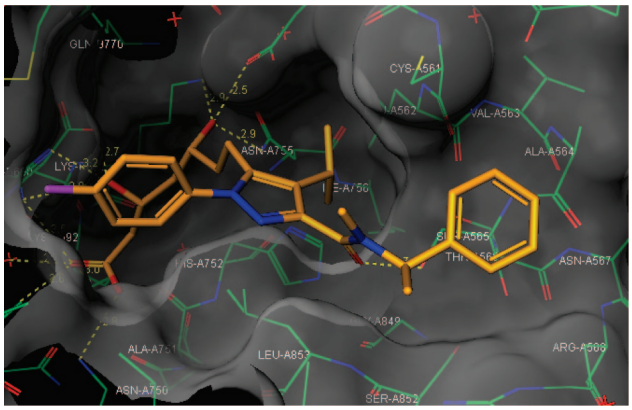

Figure 2. X-ray structure of inhibitor **50** bound to the active site of HMG-CoA reductase (2.1 Å resolution), illustrating the opportunity for installation of a conformationally restricted amide.

was a 4.5 min binary gradient of acetonitrile (containing 0.1% HCO_2H) and water (2–70%). Melting points were recorded on an Electrothermal Melting Point Apparatus and are reported uncorrected. Elemental analysis was performed at Quantitative Technologies, Inc., Whitehouse, NJ.

For experiments involving the use of animals, all procedures were carried out in compliance with the NIH Guide for the Care and Use of Laboratory Animals under a protocol approved by the Institutional (Pfizer Global Research and Development) Animal Care and Use Committee.

(4-Fluoro-phenyl)-hydrazono]-chloroacetic Acid Methyl Ester (5). To a solution of 4-fluoroaniline (10.0 g, 90.0 mmol) in MeOH (80 mL) was added 6 N HCl (80 mL), and the solution was cooled to 0 °C. $NaNO_2$ (12.4 g, 180 mmol) was then slowly added as a solid. The reaction was stirred for 15 min at 0 °C after which time NaOAc was added as a solid to adjust the reaction to pH 5. Subsequently, a solution of methyl 2-chloroacetoacetate (10.96 mL, 90.0 mmol) in MeOH (40 mL) was slowly added at 0 °C. The reaction was then allowed to warm to 25 °C and stirred for 12 h, after which time the MeOH was removed under reduced pressure and diethyl ether (300 mL) was added. The organic layer was separated and washed with saturated $NaHCO_3$ and water prior to drying over Na_2SO_4. The organic layer was concentrated to afford **5** (19.42 g, 94%), which was utilized without further purification: ^{1}H NMR ($CDCl_3$) δ 8.37 (bs, 1 H), 7.22–7.12 (m, 2 H), 7.00–6.96 (m, 2 H), 3.87 (s, 3 H); MS (APCI$^+$) *m/z* 252.9 (M + Na).

(*E*)-4-Methyl-pent-2-enoic Acid Benzyl Ester (8). To a solution of 4-methyl-2-pentenoic acid (24.0 g, 210 mmol) in acetone (300 mL) was added K_2CO_3 (55.8 g, 404 mmol), and the reaction was stirred at 25 °C for 30 min. A solution of benzyl bromide (25.2 mL, 212 mmol) in acetone (100 mL) was then added dropwise. The reaction mixture was subsequently heated to reflux for 16 h. After cooling to 25 °C, the acetone was removed under reduced pressure, ether (300 mL) and water (300 mL) were added, and the organic layer was separated, washed with brine, and dried over Na_2SO_4. After concentration, the crude product was subjected to silica gel chromatography (1–5% diethyl ether/hexanes) to afford **8** (40.5 g, 98%): ^{1}H NMR ($CDCl_3$) δ 7.36–7.28 (m, 5 H), 6.96 (dd, J = 15.6, 6.8 Hz, 1 H), 5.79 (d, J = 15.6 Hz, 1 H), 5.14 (s, 2 H), 2.42 (sept, J = 6.8 Hz, 1 H), 1.01 (d, J = 6.8 Hz, 6 H); MS (APCI$^+$) *m/z* 227.1 (M + Na).

1-(4-Fluoro-phenyl)-4-isopropyl-4,5-dihydro-1*H*-pyrazole-3,5-dicarboxylic Acid 5-Benzyl Ester 3-Methyl Ester (9). To a solution of **5** (20.93 g, 90.8 mmol) and **8** (18.54 g, 90.8 mmol) in dioxane (400 mL) at 25 °C was added Ag_2CO_3 (63.0 g, 227 mmol). The reaction was protected from light and stirred at 25 °C for 48 h. Subsequently, the reaction mixture was filtered through a pad of celite and the filtrate was concentrated. The crude product mixture was subjected to silica gel chromatography (5–20% EtOAc/hexanes) to afford **9** (29.3 g, 73%): ^{1}H NMR ($CDCl_3$) δ 7.30–7.24 (m, 3 H), 7.15–7.12 (m, 2 H), 7.01–6.96 (m, 2 H), 6.93–6.88 (m, 2 H), 5.14 (d, J = 12.4 Hz, 1 H), 5.04 (d, J = 12.4 Hz, 1 H), 4.58 (d, J = 4.0 Hz, 1 H), 3.83 (s, 3 H), 3.51–3.49 (m, 1 H), 2.40–2.36 (m, 1 H), 1.00 (d, J = 6.8 Hz, 3 H), 0.69 (d, J = 7.2 Hz, 3 H); MS (APCI$^+$) *m/z* 399.0 (M + H).

1-(4-Fluoro-phenyl)-4-isopropyl-1*H*-pyrazole-3,5-dicarboxylic Acid 5-Benzyl Ester 3-Methyl Ester (10). To a solution of **9** (29.3 g, 73.5 mmol) in THF/water (1:1, 500 mL) at 0 °C was slowly added ceric ammonium nitrate (80.5 g, 147 mmol). The reaction was stirred at 0 °C for 1 h after which time the THF was removed under reduced pressure and DCM (500 mL) was added. The organic layer was separated and washed with water and brine. The organic layer was dried over Na_2SO_4 and concentrated, and the product was purified by silica gel chromatography (5–15% EtOAc/hexanes) to provide **10** (18.95 g, 65%): ^{1}H NMR ($CDCl_3$) δ 7.29–7.21 (m, 5 H), 7.07 (d, J = 6.4 Hz, 2 H), 6.94 (t, J = 3.2 Hz, 2 H), 5.12 (s, 2 H), 3.89 (s, 3 H), 3.84 (sept, J = 7.2 Hz,1 H), 1.31 (d, J = 7.2 Hz, 6 H); MS (APCI$^+$) *m/z* 397.1 (M + H).

1-(4-Fluoro-phenyl)-5-formyl-4-isopropyl-1*H*-pyrazole-3-carboxylic Acid Methyl Ester (11). To a solution of **10** (18.95 g, 47.8 mmol) in MeOH (300 mL) at 25 °C under N_2 was added 10% Pd/C (700 mg). The reaction vessel was evacuated and filled with H_2 and then stirred at 25 °C for 3 h. Subsequently, the reaction vessel was flushed with N_2 and filtered through a pad of celite. The filtrate was concentrated to afford 1-(4-fluoro-phenyl)-4-isopropyl-1*H*-pyrazole-3,5-dicarboxylic acid 3-methyl ester (14.6g, 99%): ^{1}H NMR ($CDCl_3$) δ 7.36–7.31 (m, 2 H), 7.11–7.06 (m, 2 H), 3.90 (s, 3 H), 3.84 (sept, J = 7.2 Hz, 1 H), 1.43 (d, J = 7.2 Hz, 6 H); MS (APCI$^+$) *m/z* 307.1 (M + H).

To a solution of 1-(4-fluoro-phenyl)-4-isopropyl-1*H*-pyrazole-3,5-dicarboxylic acid 3-methyl ester (15.9 g, 51.8 mmol) in THF (300 mL) at 0 °C was slowly added BH_3·THF (1.0 M solution in THF, 104 mL, 104 mmol). The reaction was allowed to warm to 25 °C for 30 min and then heated to 65 °C for 3 h. After cooling to 25 °C, MeOH (50 mL) was slowly added. Subsequently, the solvent was removed under reduced pressure, a second portion of MeOH (100 mL) was slowly added, and the solution was stirred at 25 °C for an additional 20 min. The MeOH was then evaporated and EtOAc was added, and the organic layer was washed with 1 N NaOH and brine prior to drying over Na_2SO_4. The organic layer was concentrated and purified by silica gel chromatography (15–35% EtOAc/hexanes) to provide 1-(4-fluoro-phenyl)-5-hydroxymethyl-4-isopropyl-1*H*-pyrazole-3-carboxylic acid methyl ester (13.6 g, 90%): ^{1}H NMR ($CDCl_3$) δ 7.59–7.56 (m, 2 H), 7.15–7.11 (m, 2 H), 4.57 (s, 2 H), 3.89 (s, 3 H), 3.64 (sept, J = 7.2 Hz, 1 H), 1.36 (d, J = 7.2 Hz, 6 H); MS (APCI$^+$) *m/z* 293.1 (M + H).

To a solution of 1-(4-fluoro-phenyl)-5-hydroxymethyl-4-isopropyl-1*H*-pyrazole-3-carboxylic acid methyl ester (13.6g, 46.7 mmol) in CH_2Cl_2 (300 mL) at 25 °C was added solid $NaHCO_3$ (19.6 g, 233 mmol) followed by Dess−Martin periodinane (20.8 g, 49.0 mmol; commercially available from Lancaster). The reaction was stirred at 25 °C for 4 h after which time saturated sodium bisulfite (50 mL) was added and the organic layer was separated and washed with water and brine. The organic layer was dried over $Na_2SO_4$and concentrated to an oil that was purified by silica gel chromatography (15% EtOAc/hexanes) to afford **11** (11.3 g, 84%): ^{1}H NMR ($CDCl_3$) δ 9.95 (s, 1 H), 7.42–7.38 (m, 2 H), 7.17–7.13 (m, 2 H), 3.98 (sept, J = 7.2 Hz, 1 H), 3.92 (s, 3 H), 1.38 (d, J = 7.2 Hz, 6 H); MS (APCI$^+$) *m/z* 291.2 (M + H).

1-(4-Fluoro-phenyl)-5-formyl-4-isopropyl-1*H*-pyrazole-3-carboxylic Acid (12). To a solution of **11** (11.34 g, 39.1 mmol) in MeOH (150 mL) was added NaOH (156 mL of 1 N solution, 156 mmol). The reaction was heated to 60 °C for 4 h. The solvent was then removed under reduced pressure and water (150 mL) and Et_2O (100 mL) were added. The organic layer was discarded and the aqueous layer was acidified with 10% HCl to pH 1 and then extracted with EtOAc (200 mL × 2). The combined organic extracts were dried over Na_2SO_4 and concentrated to give **12** (8.55 g, 79%) as a white solid that required no purification: ^{1}H NMR ($CDCl_3$) δ 10.0 (s, 1 H), 7.48–7.44 (m, 2 H), 7.26–7.15 (m, 2 H), 4.02 (sept,

Table 6. LDL-Lowering Efficacy of Selected Compounds upon Chronic 7-Day Dosing

		acute inhibition of in vivo cholesterol synthesis[a]		chronic (7-day) in vivo LDL-C lowering[a]		
cmpd	structure	t = 2–4 h (10 mpk)	t = 4–6 h (10 mpk)	reduction	dose (mpk)	hepatoselectivity ratio
rosuvastatin		−76%	−46%	−42%	20	830
35	Table *2*	−74%	−15%	−41%	20	810
36	Table *2*	−71%	−19%	−42%	20	2600
39	Table *3*	−61%	−16%	−20%	20	16000
42	Table *4*	−72%	NA[b]	−15%	20	8000
48	Table *4*	−82%	−17%	−32%	10	2100
49	Table *4*	−81%	−22%	−45%	10	9500
50	Table *5*	−62%	−10%	−11%	20	6300

[a] Data represent the mean of the percent change from the control group (n = 8/group). [b] NA = not active.

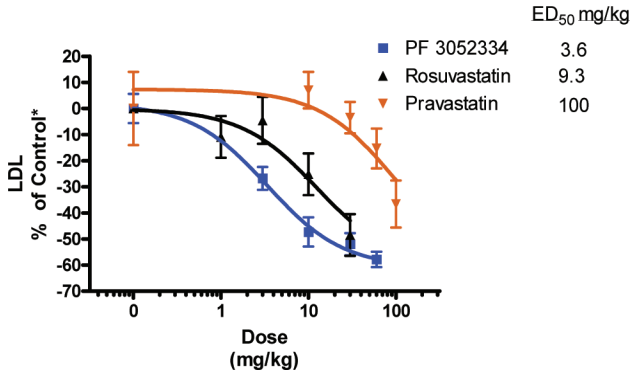

Figure 3. Comparison of PF-3052334 (**35**) versus rosuvatstatin and pravastatin in chronic plasma LDL reduction study performed in guinea pigs. Animals were dosed daily with **35**, pravastatin, or rosuvastatin for 7 days. All groups were sacrificed 2 h postdose on the final day of dosing. ED_{50} values are reported as 50% of the maximal response in LDL lowering observed in the study. Data represent the mean ± SEM of the percent change from the control group (n = 8/group).

J = 7.2 Hz, 1 H), 1.43 (d, J = 7.2 Hz, 6 H); MS ($APCI^+$) m/z 277.2 (M + H); Anal. ($C_{14}H_{13}F_1N_2O_3$) C, H, N; mp 172–174 °C.

1-(4-Fluoro-phenyl)-5-formyl-4-isopropyl-1*H*-pyrazole-3-carboxylic Acid Benzylamide (13). To a solution of **12** (1.25 g, 4.52 mmol) in CH_2Cl_2 (50 mL) at 25 °C was added 1-(3-dimethylaminopropyl)-3-ethylcarbodiimide hydrochloride (1.30 g, 6.79 mmol) followed by 1-hydroxybenzotriazole hydrate (1.04 g, 6.79 mmol), and the reaction was stirred for 5 min at 25 °C. Subsequently, benzyl amine (0.533 g, 4.98 mmol) was added, and the reaction was stirred for an additional 4 h as a fine white precipitate developed. The organic layer was washed with 1 N HCl, saturated $NaHCO_3$, and brine. After drying and concentration, the product was purified by silica gel chromatography (20% EtOAc/hexanes) to provide **13** (0.65 g, 39%): ^{1}H NMR ($CDCl_3$) δ 9.97 (s, 1 H), 7.37–7.22 (m, 7 H), 7.17–7.12 (m, 2 H), 4.57 (d, J = 6.0 Hz, 2 H), 4.15 (sept, J = 7.2 Hz, 1 H), 1.42 (d, J = 7.2 Hz, 6 H); MS ($APCI^+$) m/z 366.1 (M + H).

[5-Benzylcarbamoyl-2-(4-fluoro-phenyl)-4-isopropyl-2*H*-pyrazol-3-ylmethyl]-triphenyl-phosphonium Bromide (14). To a solution of **13** (0.620 g, 1.70 mmol) in THF/MeOH (40 mL) at 0 °C was added sodium borohydride (96.3 mg, 2.55 mmol). The reaction was stirred for 30 min at 0 °C at which point TLC analysis indicated the reaction was complete and the solvent was removed under reduced pressure. To the reaction residue was added ethyl acetate (50 mL) and saturated $NaHCO_3$ (15 mL), and the organic layer was separated, dried (Na_2SO_4), and concentrated. The resulting oil was purified by silica gel chromatography (40% EtOAc/hexanes) to afford 1-(4-fluoro-phenyl)-5-hydroxymethyl-4-isopropyl-1*H*-pyrazole-3-carboxylic acid benzylamide (0.540 g, 87%): ^{1}H NMR ($CDCl_3$) δ 7.59–7.54 (m, 2 H), 7.32–7.20 (m, 5 H), 7.15–7.10 (m, 2 H), 4.57–4.55 (m, 4 H), 3.72 (sept, J = 7.2 Hz, 1 H), 1.38 (d, J = 7.2 Hz, 6 H); MS ($APCI^+$) m/z 368.1 (M + H).

To a solution of 1-(4-fluoro-phenyl)-5-hydroxymethyl-4-isopropyl-1*H*-pyrazole-3-carboxylic acid benzylamide (0.525 g, 1.43 mmol) in acetonitrile (50 mL) was added triphenylphosphine hydrobromide (0.49 g, 1.43 mmol). The reaction was heated to 80 °C for 48 h after which time all starting material was consumed as determined by TLC. The reaction solvent was removed under reduced pressure and the resulting white solid was dried under high vacuum for 12 h to provide **14** (0.977 g, 98%) in sufficient purity for use in the next step.

(6-{2-[5-Benzylcarbamoyl-2-(4-fluoro-phenyl)-4-isopropyl-2*H*-pyrazol-3-yl]-vinyl}-2,2-dimethyl-[1*R*,3*R*]dioxan-4-yl)-acetic Acid *tert*-Butyl Ester (17). To a solution of **14** (0.562 g, 0.811 mmol) in THF/DMSO (50:1, 50 mL) at −78 °C was added 1.0 M LiHMDS (1.055 mL, 1.055 mmol). An orange color was noted as the base was added. The reaction mixture was stirred at −78 °C for 5 min after which time a solution of **16** in THF (10 mL) was slowly added. After the addition, the reaction mixture was stirred at −78 °C for 30 min, then allowed to warm to 25 °C, and stirred at that temperature for 5 h. The reaction was quenched by dropwise addition of saturated NH_4Cl. Ethyl acetate (50 mL) was then added and the organic layer was separated, washed with water, dried (Na_2SO_4), and concentrated. The crude product was purified by silica gel chromatography (15–20% EtOAc/hexanes) to afford **17** as an inseparable 1:4 mixture of *cis*/*trans*-olefin isomers.

To a solution of **17** (0.360 g, 0.61 mmol) in MeOH (20 mL) was added 1 N HCl (2 mL), and the solution was stirred for 3 h at 25 °C. Subsequently, the reaction solvent was removed under reduced pressure and ethyl acetate (50 mL) and saturated $NaHCO_3$ (10 mL) were added. The organic layer was separated, washed with brine, dried (Na_2SO_4), and concentrated to afford, after silica gel chromatography (35% EtOAc/hexanes), 7-[5-benzylcarbamoyl-2-(4-fluoro-phenyl)-4-isopropyl-2*H*-pyrazol-3-yl]-3,5-dihydroxy-hept-6-enoic acid *tert*-butyl ester (0.231 g, 69%) as a mixture of *cis*/*trans*-isomers.

Subsequently, to a solution of 7-[5-benzylcarbamoyl-2-(4-fluoro-phenyl)-4-isopropyl-2*H*-pyrazol-3-yl]-3,5-dihydroxy-hept-6-enoic acid *tert*-butyl ester (0.241 g, 0.437 mmol) in MeOH (20 mL) was added 10% Pd/C (50 mg), and the reaction vessel was evacuated and filled with hydrogen gas (via balloon) for 3 h. The reaction mixture was then filtered through a pad of celite. The crude product was purified by silica gel chromatography (30–50% EtOAc/hexanes) to afford **18** (0.143 g, 59%): ^{1}H NMR ($CDCl_3$) δ 7.38–7.23 (m, 7 H), 7.16–7.12 (m, 2 H), 4.57 (d, J = 6.4 Hz, 2 H), 4.13–4.08 (m, 1 H), 3.73–3.72 (m, 1 H), 3.41–3.37 (m, 2 H), 2.83–2.80 (m, 1 H), 2.69–2.67 (m, 1 H), 1.44 (s, 9 H), 1.39 (d, J = 7.2 Hz, 6 H), 1.51–1.22 (m, 6 H); MS ($APCI^+$) m/z 554.3 (M + H).

(3*R*,5*R*)-7-[5-Benzylcarbamoyl-2-(4-fluoro-phenyl)-4-isopropyl-2*H*-pyrazol-3-yl]-3,5-dihydroxy-heptanoic Acid Sodium Salt (2). To a solution of **18** (0.103 g, 0.186 mmol) in MeOH (5 mL) was added 1.0 N NaOH (0.190 mL, 0.195 mmol), and the reaction was stirred at 25 °C for 48 h after which time the reaction solvent was removed under reduced pressure. The resulting solid was then azeotroped with toluene (3 × 100 mL) and triturated with diethyl ether to provide a light yellow solid that was dried under vacuum at 60 °C to afford **2** (0.091 g, 94%): ^{1}H NMR (DMSO-d_6) δ 8.55 (t, J = 2.4 Hz, 1 H), 7.53–7.49 (m, 2 H), 7.33–7.13 (m, 7 H), 4.70 (bs, 1 H), 4.34 (d, J = 6.4 Hz, 2 H), 3.63–3.57 (m, 1 H), 3.45–3.42 (m, 1 H), 2.74–2.66 (m, 1 H), 2.58–2.50 (m, 1 H), 1.92 (dd, J = 14.8, 4.0 Hz, 1 H), 1.72 (dd, J = 15.2, 8.0 Hz, 1 H), 1.40–1.10 (m,

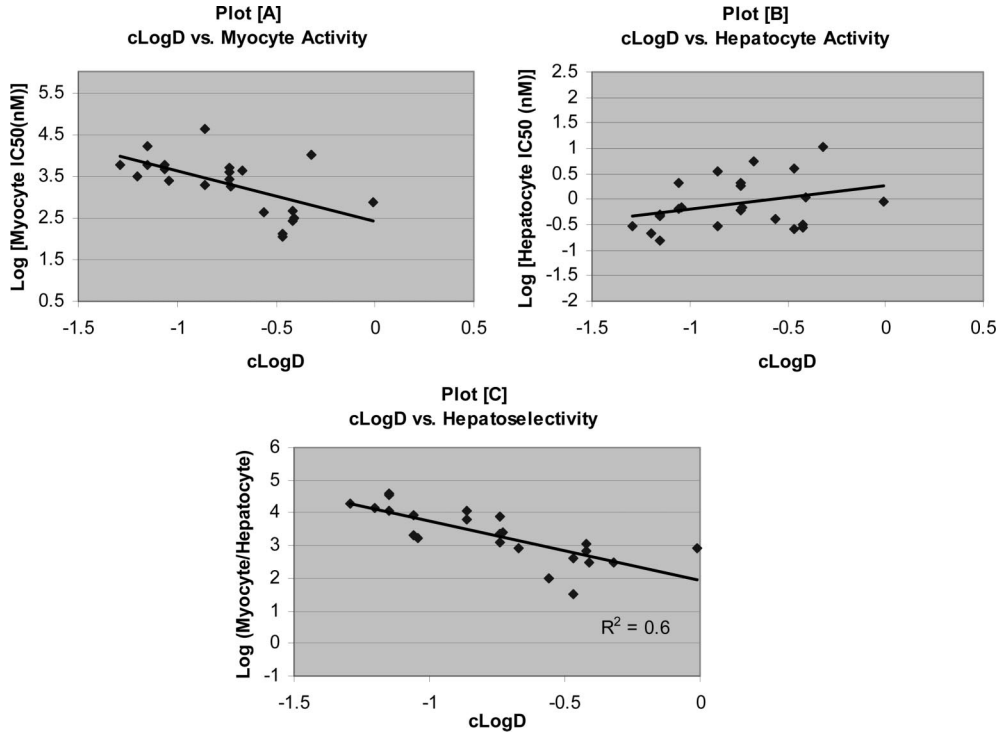

Figure 4. Relationships between predicted lipophilicity and myocyte activity [Plot A], hepatocyte activity [Plot B], and hepatoselectivity [Plot C].

10 H); HRMS (ESI) calcd for $C_{27}H_{32}FN_3O_5$ [$(M + H)^+$], 498.2399; found, 498.2393; HPLC (method B) $t_R = 1.86$ min (98.2%).

5-(Benzylcarbamoyl)-1-(4-fluorophenyl)-4-isopropyl-1*H*-pyrazole-3-carboxylic Acid (21). To a solution of **10** (9.40 g, 23.7 mmol) in MeOH (150 mL) at 25 °C under N_2 was added 10% Pd/C (500 mg). The reaction vessel was evacuated and filled with H_2 and then stirred at 25 °C for 3 h. Subsequently, the reaction vessel was flushed with N_2 and filtered through a pad of celite. The filtrate was concentrated to afford **19** (7.20 g, 99%).

To a solution of **19** (3.00 g, 9.79 mmol) in CH_2Cl_2 (100 mL) at 25 °C was added 1-(3-dimethylaminopropyl)-3-ethylcarbodiimide hydrochloride (2.82 g, 14.7 mmol) followed by 1-hydroxybenzotriazole hydrate (2.25 g, 14.7 mmol), and the reaction was stirred for 5 min at 25 °C. Subsequently, benzyl amine (1.26 g, 11.8 mmol) was added, and the reaction was stirred for an additional 8 h. The organic layer was washed with 1 N HCl, saturated $NaHCO_3$, and brine. After drying and concentration, the product was purified by silica gel chromatography (15% EtOAc/hexanes) to provide **20** (2.20 g, 57%).

To a solution of **20** (2.20 g, 5.56 mmol) in MeOH (50 mL) was added NaOH (22.3 mL of 1 N solution, 22.3 mmol). The reaction was heated to 60 °C for 3 h. The solvent was then removed under reduced pressure and water (50 mL) and Et_2O (100 mL) were added. The organic layer was discarded and the aqueous layer was acidified with 10% HCl to pH 1 and then extracted with EtOAc (200 mL × 2). The combined organic extracts were dried over Na_2SO_4 and concentrated to give **21** (2.07 g, 98%) as a white solid that required no purification: ^{1}H NMR ($CDCl_3$) δ 7.45–7.41 (m, 2 H), 7.25–7.21 (m, 3 H), 7.06–7.01 (m, 4 H), 5.86 (bs, 1 H), 4.42 (d, $J = 5.6$ Hz, 2 H), 3.55 (sept, $J = 7.2$ Hz, 1 H), 1.31 (d, $J = 7.2$ Hz, 6 H).

***N*-Benzyl-1-(4-fluorophenyl)-3-(hydroxymethyl)-4-isopropyl-1*H*-pyrazole-5-carboxamide (22).** To a solution of **21** (2.07 g, 5.43 mmol) in THF (100 mL) at 0 °C was slowly added $BH_3 \cdot$THF (8.14 mL of 1.0 M solution in THF, 8.14 mmol). The reaction was allowed to warm to 25 °C for 30 min and then heated to 65 °C for 4 h. After cooling to 25 °C, MeOH (20 mL) was slowly added. Subsequently, the solvent was removed under reduced pressure, a second portion of MeOH (50 mL) was slowly added, and the solution was stirred at 25 °C for an additional 20 min. The MeOH was then evaporated, EtOAc was added, and the organic layer was washed with 1 N NaOH and brine prior to drying over Na_2SO_4. The organic layer was concentrated and purified by silica gel chromatography (15–35% EtOAc/hexanes) to provide **22** (0.69 g, 35%): MS(APCI$^+$) *m*/*z* 368.1 (M + H).

(3*R*,5*R*)-*tert*-Butyl 7-(5-(benzylcarbamoyl)-1-(4-fluorophenyl)-4-isopropyl-1*H*-pyrazol-3-yl)-3,5-dihydroxyheptanoate (25). To a solution of **22** (0.69 g, 1.88 mmol) in CH_2Cl_2 (50 mL) at 25 °C was slowly added PBr_3 (0.94 mL of 1.0 M solution in CH_2Cl_2, 0.94 mmol). The resulting reaction mixture was then stirred at 25 °C for 12 h, after which time water (10 mL) was added, and the reaction mixture was stirred for an additional 0.5 h at 25 °C. The organic layer was separated, washed with saturated $NaHCO_3$ solution (2 × 40 mL), washed with brine (1 × 40 mL), dried (Na_2SO_4), and concentrated to afford *N*-benzyl-3-(bromomethyl)-1-(4-fluorophenyl)-4-isopropyl-1*H*-pyrazole-5-carboxamide (0.810 g, 100%), which was utilized without additional purification.

To a solution of *N*-benzyl-3-(bromomethyl)-1-(4-fluorophenyl)-4-isopropyl-1*H*-pyrazole-5-carboxamide (0.810 g, 1.88 mmol) in toluene (50 mL) at 25 °C was added triphenyl phosphine (0.494 g, 1.88 mmol). The resulting reaction mixture was then heated to 80 °C for 14 h. The reaction mixture was then cooled to 25 °C, the solvent was removed under reduced pressure, CH_2Cl_2 (100 mL) was added, and the solution was concentrated under reduced pressure to afford **23** (1.30 g, 100%), which was utilized without additional purification.

To a solution of **23** (1.30 g, 1.88 mmol) in THF (50 mL) at −78 °C was added 1.0 M LiHMDS (2.44 mL, 2.44 mmol). The reaction mixture was stirred at −78 °C for 5 min, after which time a solution of **16** (0.582 g, 2.25 mmol) in THF (10 mL) was slowly added. After the addition, the reaction mixture was stirred at −78 °C for 30 min then allowed to warm to 25 °C and stirred at that temperature for 2 h. The reaction was quenched by dropwise addition of saturated NH_4Cl. Ethyl acetate (75 mL) was then added, and organic layer was separated, washed with water, dried (Na_2SO_4), and concentrated. The crude product was purified by silica gel chromatography (10% EtOAc/hexanes) to afford **24** (0.70 g, 63%) as an inseparable about 1:3 mixture of *cis*/*trans*-olefin isomers.

To a solution of **24** (0.70 g, 1.18 mmol) in MeOH (15 mL) was added 1 N HCl (2 mL), and the solution was stirred for 1.5 h at 25 °C. Subsequently, the reaction solvent was removed under reduced

pressure and ethyl acetate (50 mL) and saturated $NaHCO_3$ solution (15 mL) were added. The organic layer was separated, washed with brine, dried (Na_2SO_4), and concentrated to afford, after silica gel chromatography (40% EtOAc/hexanes), (3*R*,5*R*)-*tert*-butyl 7-(5-(benzylcarbamoyl)-1-(4-fluorophenyl)-4-isopropyl-1*H*-pyrazol-3-yl)-3,5-dihydroxyhept-6-enoate (0.65 g, 93%) as a mixture of *cis*/*trans*-isomers.

Subsequently, to a solution of (3*R*,5*R*)-*tert*-butyl 7-(5-(benzylcarbamoyl)-1-(4-fluorophenyl)-4-isopropyl-1*H*-pyrazol-3-yl)-3,5-dihydroxyhept-6-enoate (0.605 g, 1.10 mmol) in MeOH (15 mL) was added 10% Pd/C (70 mg), and the reaction vessel was evacuated and filled with hydrogen gas (via balloon) for 4 h. The reaction mixture was then filtered through a pad of celite. The crude product was purified by silica gel chromatography (45% EtOAc/hexanes) to **25** (0.34 g, 56%): ^{1}H NMR ($CDCl_3$) δ 7.34–7.30 (m, 2 H), 7.23–7.19 (m, 3 H), 7.01–6.93 (m, 4 H), 5.86 (t, J = 5.6 Hz, 1 H), 4.42 (d, J = 6.0 Hz, 2 H), 4.18–4.16 (m, 1 H), 3.92–3.88 (m, 1 H), 3.01 (sept, J = 6.8 Hz, 1 H), 2.75 (t, J = 7.6 Hz, 2 H), 2.34–2.32 (m, 1 H), 1.84–1.79 (m, 2 H), 1.58–1.54 (m, 2 H), 1.40 (s, 9 H), 1.24 (d, J = 6.8 Hz, 6 H); MS (APCI$^+$) *m*/*z* 554.2 (M + H).

(3*R*,5*R*)-7-(5-(Benzylcarbamoyl)-1-(4-fluorophenyl)-4-isopropyl-1*H*-pyrazol-3-yl)-3,5-dihydroxyheptanoic Acid Sodium Salt (3). To a solution of **25** (0.428 g, 0.773 mmol) in MeOH (5 mL) was added 1.0 N NaOH (0.788 mL, 0.788 mmol), and the reaction was stirred at 25 °C for 16 h after which time the reaction was solvent was removed under reduced pressure. The resulting solid was then azeotroped with toluene (2 × 50 mL) to provide a white solid that was dried under vacuum at 60 °C to afford **3** (0.39 g, 97%): ^{1}H NMR (DMSO-d_6) δ 7.55 (s, 1 H), 7.36–7.33 (m, 2 H), 7.21–7.05 (m, 7 H), 4.69 (bs, 1 H), 3.70–3.63 (m, 2 H), 3.15 (sept, J = 7.2 Hz, 1 H), 3.71–3.59 (m, 1 H), 3.51–3.41 (m, 1 H), 1.93 (dd, J = 14.8, 3.6 Hz, 1 H), 1.79–1.25 (m, 5 H), 1.14 (d, J = 7.2 Hz, 6 H); HRMS (ESI) calcd for $C_{27}H_{32}FN_3O_5$ [(M + H)$^+$], 498.2399; found, 498.2397; HPLC (method A) t_R = 6.57 min (98.2%).

1-(4-Fluoro-phenyl)-5-formyl-4-isopropyl-1*H*-pyrazole-3-carboxylic Acid Methyl-(2-methyl-benzyl)-amide (26). To a solution of 2-methylbenzaldehyde (10.0 g, 83.23 mmol) in MeOH at 25 °C was added methylamine (40% in H_2O, 25.85 g, 332.9 mmol). The reaction mixture was stirred at 25 °C for 30 min, after which time it was cooled to 0 °C and $NaBH_4$ (6.30 g, 166.5 mmol) was added portionwise. The reaction mixture was then warmed to 25 °C and stirred for an additional 1 h. The solvent was removed under reduced pressure, and water and CH_2Cl_2 were added. The organic layer was separated and washed with saturated $NaHCO_3$ and brine. After drying over Na_2SO_4, the organic phase was concentrated to afford the desired methyl-(2-methyl-benzyl)-amine (10.49 g, 93.2%) as an oil of sufficient purity for use in the next reaction: ^{1}H NMR ($CDCl_3$) δ 7.35–7.08 (m, 3 H), 3.73 (s, 2 H), 2.49 (s, 3 H), 2.34 (s, 3 H); MS (APCI$^+$) 136.3 *m*/*z* (M + H).

To a solution of **12** (1.50 g, 5.43 mmol) in CH_2Cl_2 (100 mL) at 25 °C was added EDCI (1.56 g, 8.14 mmol), followed by HOBt·H_2O (1.25 g, 8.14 mmol), and the reaction was stirred for 10 min at 25 °C. Subsequently, methyl-(2-methyl-benzyl)-amine (1.10 g, 8.14 mmol) was added, and the reaction was stirred for an additional 6 h at 25 °C. The organic layer was then washed with HCl, saturated $NaHCO_3$, and brine. After drying over Na_2SO_4 and concentrated, the product was purified by column chromatography (10–25% EtOAc/hexanes) to afford **26** (1.53 g, 71.6%) as an oil: ^{1}H NMR ($CDCl_3$) [mixture of rotamers at 25 °C] δ 9.36 (s), 9.14 (s), 7.44–7.40 (m), 7.31–7.11 (m) 4.80 (s), 4.65 (s), 3.56 (sept), 3.04 (s), 2.89 (s) 2.35 (s), 2.19 (s), 1.40–1.38 (m); MS (APCI$^+$) 394.2 *m*/*z* (M + H).

7-{2-(4-Fluoro-phenyl)-4-isopropyl-5-[methyl-(2-methyl-benzyl)-carbamoyl]-2*H*-pyrazol-3-yl}-5-hydroxy-3-oxo-hept-6-enoic Acid Methyl Ester (29). To a solution of **26** (1.53 g, 3.89 mmol) in toluene (80 mL) was added 3-(*tert*-butyl-dimethyl-silanyloxy)-5-oxo-6-(triphenyl-l5-phosphanylidene)-hexanoic acid methyl ester[22] (2.70 g, 5.06 mmol), and the reaction was heated to 95 °C for 16 h. After cooling to 25 °C, the solvent was removed under reduced pressure and the product was run through pad of silica gel (20–30% EtOAc/hexanes) to afford **28** (2.48 g, 98.1%). To a solution of **28** (2.48 g, 3.82 mmol) in MeCN (40 mL) at 25 °C was added HF (2.5 mL of 48% in water). The reaction was stirred at 25 °C for 16 h. Subsequently, EtOAc (100 mL) and water (100 mL) were added, and the organic layer was separated, dried, and concentrated. Product was purified by column chromatography (30–50% EtOAc−hexanes) to afford **29** (2.03 g, 98.0%): ^{1}H NMR ($CDCl_3$) [mixture of rotamers at 25 °C] δ 7.41–7.43 (m), 7.33–7.09 (m), 6.26 (d), 6.20 (d), 4.74 (s), 4.66 (s), 4.49 (bs), 3.69 (s), 3.38–3.37 (m), 3.17–3.13 (m), 3.03 (s), 2.91 (s), 2.76–2.74 (m), 2.54–2.53 (m), 2.35 (s), 2.31 (s), 1.39–1.36 (m), 1.24–1.22 (m); MS (APCI$^+$) 536.4 *m*/*z* (M + H).

7-{2-(4-Fluoro-phenyl)-4-isopropyl-5-[methyl-(2-methyl-benzyl)-carbamoyl]-2*H*-pyrazol-3-yl}-3,5-dihydroxy-hept-6-enoic Acid Methyl Ester (30). To a solution of **29** (2.04 g, 3.81 mmol) in THF (100 mL) and MeOH (30 mL) at −78 °C was added diethylmethoxyborane (4.95 mL of 1.0 M solution, 4.95 mmol). The reaction was stirred at −78 °C for 1 h, after which time $NaBH_4$ (166 mg, 4.38 mmol) was added. The reaction mixture was stirred at −78 °C for 2 h and then warmed to 0 °C, after which time glacial acetic acid (0.5 mL) was added. The reaction was diluted with EtOAc and water, and the organic layer was separated and washed with satd $NaHCO_3$ and brine prior to concentration. The resulting crude oil was then dissolved in MeOH (50 mL) and evaporated again. Subsequently, a second amount of MeOH (50 mL) was added and the solution was stirred at 25 °C for 12 h, after which time it was concentrated and purified by column chromatography (40–60% EtOAc/hexanes) to afford **30** (1.66 g, 81.1%): ^{1}H NMR ($CDCl_3$) [mixture of rotamers at 25 °C] δ 7.40–7.36 (m), 7.30–7.03 (m), 6.44 (d), 5.79 (dd), 5.70 (dd), 4.78 (s), 4.70 (s), 4.51–4.44 (m), 4.27–4.24 (m), 3.71 (s), 3.68–3.54 (m), 3.05 (sept), 3.01 (s), 2.92 (s), 2.52–2.49 (m), 2.35 (s), 2.25 (s), 1.71–1.52 (m), 1.37–1.31 (m); MS (APCI$^+$) 538.2 *m*/*z* (M + H).

7-{2-(4-Fluoro-phenyl)-4-isopropyl-5-[methyl-(2-methyl-benzyl)-carbamoyl]-2*H*-pyrazol-3-yl}-3,5-dihydroxy-heptanoic Acid Methyl Ester (31). To a solution of **30** (1.19 g, 2.21 mmol) in MeOH (50 mL) was added Pd/C (100 mg). The reaction vessel was evacuated, flushed with nitrogen, and then filled with hydrogen (via balloon). The reaction was stirred at 25 °C for 4 h, then flushed with nitrogen, and filtered through a pad of celite. The filtrate was concentrated and purified by column chromatography (30–40% EtOAc/hexanes) to afford **31** (0.792 g, 66%): ^{1}H NMR ($CDCl_3$) [mixture of rotamers at 25 °C] δ 7.39–7.36 (m), 7.29–7.07 (m), 5.28 (s), 4.77 (s), 4.71 (s), 4.18–4.11 (m), 3.79–3.71 (m), 3.69 (s), 3.15–3.05 (m), 3.04–2.78 (m), 2.76–2.61 (m), 2.43 (s), 2.40 (s), 2.35 (s), 2.20 (s), 1.53–1.16 (m); MS (APCI$^+$) 540.2 *m*/*z* (M + H).

(3*R*,5*R*)-7-{2-(4-Fluoro-phenyl)-4-isopropyl-5-[methyl-(2-methyl-benzyl)-carbamoyl]-2*H*-pyrazol-3-yl}-3,5-dihydroxy-heptanoic Acid Sodium Salt (32). To a solution of **31** (0.792 g, 1.47 mmol) in MeOH (5 mL), NaOH solution (1.028 N, 1.50 mL, 1.54 mmol) was added. The reaction mixture was stirred at 25 °C for 12 h. After the solvent was evaporated, the crude product was dried azeotopically with toluene (3 × 10 mL). It was dissolved in a MeOH/CH_2Cl_2 mixture (1:9, 10 mL) and diluted with CH_2Cl_2 (15 mL). It was filtered through cotton, and the filtrate was concentrated and triturated with Et_2O for 12 h. The product was isolated by filtration and dried under vacuum at 60 °C for 12 h to afford **32** (798 mg, 99%): ^{1}H NMR (DMSO-d_6) [mixture of rotamers at 25 °C] δ 7.79–7.65 (m), 7.58–7.46 (m), 7.41–7.24 (m), 7.22–7.07 (m), 4.85–4.60 (m), 3.62–3.58 (m), 3.46–3.44 (m), 2.89–2.85 (m), 2.84 (s), 2.74–2.66 (m), 2.54–2.45 (m), 2.29 (s), 1.93–1.88 (m), 1.73–1.67 (m), 1.53–1.10 (m); HRMS (ESI) calcd for $C_{29}H_{36}FN_3O_5$ [(M + H)$^+$], 526.2712; found, 526.2703; HPLC (method A) t_R = 7.39 min (95.4%).

(3*R*,5*R*)-7-[2-(4-Fluoro-phenyl)-4-isopropyl-5-(4-methoxy-benzylcarbamoyl)-2*H*-pyrazol-3-yl]-3,5-dihydroxy-heptanoic Acid Sodium Salt (33). ^{1}H NMR (DMSO-d_6) δ 7.51–7.48 (m, 2 H), 7.32–7.28 (m, 2 H), 7.21–7.16 (m, 3 H), 6.80 (d, J = 8.8 Hz, H), 4.27 (s, 2 H), 3.65 (s, 3 H), 3.64–3.49 (m, 3 H), 2.73–2.69 (m, 1 H), 2.57–2.49 (m, 1 H), 1.94 (dd, J = 14.8, 4.0 Hz, 1 H), 1.74 (dd,

J = 14.8, 8.4 Hz, 1 H), 1.24 (d, J = 7.2 Hz, 6 H), 1.37–1.10 (m, 4 H); HRMS (ESI) calcd for $C_{28}H_{34}FN_3O_5$ [(M + H)$^+$], 528.2504; found, 528.2454; HPLC (method B) t_R = 1.76 min (>99%).

(3*R*,5*R*)-7-[2-(4-Fluoro-phenyl)-4-isopropyl-5-(4-fluoro-benzylcarbamoyl)-2*H*-pyrazol-3-yl]-3,5-dihydroxy-heptanoic Acid Sodium Salt (34). ^{1}H NMR (DMSO-d_6) δ 7.52–7.48 (m, 2 H), 7.32–7.26 (m, 4 H), 7.06 (t, J = 8.8 Hz, 2 H), 4.31 (s, 2 H), 3.61–3.58 (m, 1 H), 3.45–3.42 (m, 1 H), 3.23–3.11 (m, 1 H), 2.73–2.61 (m, 1 H), 2.57–2.49 (m, 1 H), 1.89 (dd, J = 14.8, 4.0 Hz, 1 H), 1.67 (dd, J = 14.8, 8.4 Hz, 1 H), 1.24 (d, J = 7.2 Hz, 6 H), 1.35–1.05 (m, 4 H); HRMS (ESI) calcd for $C_{27}H_{31}F_2N_3O_5$ [(M + H)$^+$], 516.2305; found, 516.2309; HPLC (method B) t_R = 1.91 min (>99%).

(3*R*,5*R*)-7-[2-(4-Fluoro-phenyl)-4-isopropyl-5-(4-methyl-benzylcarbamoyl)-2*H*-pyrazol-3-yl]-3,5-dihydroxy-heptanoic Acid Sodium Salt (35). ^{1}H NMR (DMSO-d_6) δ 7.52–7.48 (m, 2 H), 7.29 (t, J = 8.8 Hz, 2 H), 7.14 (J = 8.0 Hz, 2 H), 7.03 (d, J = 8.0 Hz, 2 H), 4.29 (s, 2 H), 3.62–3.56 (m, 1 H), 3.45–3.42 (m, 1 H), 3.28 (bs, 1 H), 2.73–2.66 (m, 1 H), 2.57–2.51 (m, 1 H), 2.20 (s, 3 H), 1.90 (dd, J = 14.8, 4.0 Hz, 1 H), 1.70 (dd, J = 14.8, 8.4 Hz, 1 H), 1.24 (d, J = 7.2 Hz, 6 H), 1.53–1.11 (m, 4 H); MS (APCI$^+$) m/z 512.2 (M + H); Anal. ($C_{28}H_{33}F_1N_3O_5Na$) C, H, N; HPLC (method A) t_R = 8.29 min (99.5%); mp 240–241 °C.

(3*R*,5*R*)- 7-[2-(4-Fluoro-phenyl)-4-isopropyl-5-(3-methoxymethyl-benzylcarbamoyl)-2*H*-pyrazol-3-yl]-3,5-dihydroxy-heptanoic Acid Sodium Salt (36). ^{1}H NMR (DMSO-d_6) δ 8.56 (t, J = 6.0 Hz, 1 H), 7.55–7.52 (m, 2 H), 7.35–7.11 (m, 6 H), 4.73 (bs, 1 H), 4.37–4.33 (m, 4 H), 3.64–3.62 (m, 1 H), 3.48–3.46 (m, 1 H), 3.23 (s, 3 H), 2.72–2.69 (m, 1 H), 2.59–2.45 (m, 1 H), 1.95 (dd, J = 14.8, 4.0 Hz, 1 H), 1.73 (dd, J = 14.8, 8.0 Hz, 1 H), 1.40–1.26 (d, J = 6.8 Hz, 6 H), 1.41–1.13 (m, 4 H); HRMS (ESI) calcd for $C_{29}H_{36}FN_3O_6$ [(M + H)$^+$], 542.2661; found, 542.2649; Anal. ($C_{28}H_{33}FN_3O_5Na\cdot 0.6\ H_2O$) C, H, N; HPLC (method A) t_R = 7.13 min (98.2%).

(3*R*,5*R*)-7-[5-(3-Cyano-benzylcarbamoyl)-2-(4-fluoro-phenyl)-4-isopropyl-2*H*-pyrazol-3-yl]-3,5-dihydroxy-heptanoic Acid Sodium Salt (37). ^{1}H NMR (DMSO-d_6) δ 8.78–8.75 (m, 1 H), 7.77–7.60 (m, 2 H), 7.59–7.40 (m, 4 H), 7.38–7.23 (m, 2 H), 4.76–4.72 (m, 1 H), 4.43–4.38 (m, 2 H), 3.68–3.58 (m, 1 H), 3.57–3.42 (m, 1 H), 3.23–3.16 (m, 2 H), 2.80–2.62 (m, 1 H), 2.61–2.50 (m, 1 H), 1.93 (dd, J = 14.8, 4.0 Hz, 1 H), 1.73 (dd, J = 14.8, 8.4 Hz, 1 H), 1.26 (d, J = 6.8 Hz, 6 H), 1.43–1.08 (m, 4 H); HRMS (ESI) calcd for $C_{28}H_{31}FN_4O_5$ [(M + H)$^+$], 523.2351; found, 523.2344; HPLC (method A) t_R = 6.91 min (98.0%).

(3*R*,5*R*)-7-[5-(4-Dimethylcarbamoyl-benzylcarbamoyl)-2-(4-fluoro-phenyl)-4-isopropyl-2*H*-pyrazol-3-yl]-3,5-dihydroxy-heptanoic Acid Sodium Salt (38). ^{1}H NMR (DMSO-d_6) δ 8.64–8.59 (m, 1 H), 7.67–7.35 (m, 4 H), 7.30–7.05 (m, 4 H), 4.72 (s, 1 H), 4.36 (d, J = 6.0 Hz, 2 H), 3.65–3.35 (m, 2 H), 2.90 (s, 3 H), 2.82 (s, 3 H), 1.88 (dd, J = 14.8, 4.0 Hz, 1 H), 1.66 (dd, J = 14.8, 8.2 Hz, 1 H), 1.23 (d, J = 6.8 Hz, 6 H), 1.40–1.05 (m, 4 H); HRMS (ESI) calcd for $C_{30}H_{37}FN_4O_5$ [(M + H)$^+$], 569.2769; found, 569.2778; HPLC (method C) t_R = 2.14 min (>99%).

(3*R*,5*R*)-7-[5-(Benzyl-methyl-carbamoyl)-2-(4-fluoro-phenyl)-4-isopropyl-2*H*-pyrazol-3-yl]-3,5-dihydroxy-heptanoic Acid Sodium Salt (39). ^{1}H NMR (DMSO-d_6) δ 7.42–7.06 (m, 9 H), 4.61 (s, 1 H), 4.49 (s, 1 H), 3.87–3.71 (m, 4 H), 3.47–3.42 (m, 1 H), 2.80–2.69 (m, 3 H), 1.95 (dd, J = 14.8, 4.0 Hz, 1 H), 1.77 (dd, J = 14.8, 7.6 Hz, 1 H), 1.17 (d, J = 7.2 Hz, 6), 1.57–1.21 (m, 4 H); HRMS (ESI) calcd for $C_{28}H_{34}FN_3O_5$ [(M + H)$^+$], 512.2555; found, 512.2545; Anal. ($C_{28}H_{33}FN_3O_6Na$) C, H, N; HPLC (method A) t_R = 6.79 min (98.2%).

(3*R*,5*R*)- 7-[5-(Benzyl-ethyl-carbamoyl)-2-(4-fluoro-phenyl)-4-isopropyl-2*H*-pyrazol-3-yl]-3,5-dihydroxy-heptanoic Acid Sodium Salt (40). ^{1}H NMR (DMSO-d_6) δ 7.47–7.21 (m, 9 H), 4.71 (bs, 1 H), 4.62 (s, 1 H), 4.47 (s, 1 H), 3.76–3.74 (m, 1 H), 3.59–3.56 (m, 1 H), 3.29–3.17 (m, 2 H), 2.87–2.85 (m, 1 H), 2.71–2.67 (m, 1 H), 2.57–2.52 (m, 1 H), 1.90 (dd, J = 14.8, 4.0 Hz, 1 H), 1.70 (dd, J = 14.8, 8.0 Hz, 1 H), 1.41–1.19 (m, 4 H), 1.16 (d, J = 6.8 Hz, 6 H), 1.00 (t, J = 5.2 Hz, 3 H); HRMS (ESI) calcd for $C_{29}H_{36}FN_3O_5$ [(M + H)$^+$], 526.2712; found, 526.2687; HPLC (method C) t_R = 3.15 min (98.0%).

(3*R*,5*R*)- 7-[5-(Benzyl-isopropyl-carbamoyl)-2-(4-fluoro-phenyl)-4-isopropyl-2*H*-pyrazol-3-yl]-3,5-dihydroxy-heptanoic Acid Sodium Salt (41). ^{1}H NMR (DMSO-d_6) δ 7.66–7.59 (m, 2 H), 7.48–7.19 (m, 7 H), 4.71 (bs, 1 H), 4.56 (s, 1 H), 4.44 (s, 1 H), 3.83–3.81 (m, 1 H), 3.46–3.43 (m, 1 H), 3.27–3.19 (m, 1 h), 2.90–2.88 (m, 1 H), 2.79–2.72 (m, 1 H), 2.65–2.60 (m, 1 H), 1.91 (dd, J = 14.8, 4.0 Hz, 1 H), 1.70 (dd, J = 14.8, 8.4 Hz, 1 H), 1.41–1.21 (m, 4 H), 1.18 (d, J = 6.0 Hz, 6 H), 1.02 (d, J = 6.8 Hz, 6 H); HRMS (ESI) calcd for $C_{30}H_{38}FN_3O_5$ [(M + H)$^+$], 540.2868; found, 540.2847; HPLC (method C) t_R = 3.34 min (95.2%).

(3*R*,5*R*)- 7-{2-(4-Fluoro-phenyl)-4-isopropyl-5-[methyl-(3-methyl-benzyl)-carbamoyl]-2*H*-pyrazol-3-yl}-3,5-dihydroxy-heptanoic Acid Sodium Salt (42). ^{1}H NMR (DMSO-d_6) δ 7.47–7.41 (m, 2 H), 7.31–7.27 (m, 1 H), 7.21–7.07 (m, 5 H), 4.71 (bs, 1 H), 4.58 (s, 1 H), 4.47 (s, 1 H), 3.61–3.59 (m, 1 H), 3.46–3.43 (m, 1 H), 2.89–2.87 (m, 1 H), 2.80 (s, 3 H), 2.78–2.75 (m 1 H), 2.56–2.52 (m, 1 H), 2.21 (s, 3 H), 1.91 (dd, J = 14.8, 4.0 Hz, 1 H), 1.69 (dd, J = 14.8, 8.2 Hz, 1 H), 1.36–1.10 (m, 4 H), 1.16 (d, J = 6.8 Hz, 6 H); HRMS (ESI) calcd for $C_{29}H_{36}FN_3O_5$ [(M + H)$^+$], 526.2712; found, 526.2702; HPLC (method C) t_R = 3.67 min (>99%).

(3*R*,5*R*)-7-{2-(4-Fluoro-phenyl)-4-isopropyl-5-[methyl-(4-methyl-benzyl)-carbamoyl]-2*H*-pyrazol-3-yl}-3,5-dihydroxy-heptanoic Acid Sodium Salt (43). ^{1}H NMR (DMSO-d_6) δ 7.47–7.41 (m, 2 H), 7.31–7.25 (m, 2 H), 7.18–7.06 (m, 4 H), 4.71 (bs, 1 H), 4.57 (s, 1 H), 4.45 (s, 1 H), 3.65–3.61 (m, 1 H), 3.45–3.42 (m, 1 H), 2.88–2.85 (m, 1 H), 2.78 (s, 3 H), 2.77–2.72 (m, 1 H), 2.55–2.52 (m, 1 H), 2.22–2.20 (m, 3 H), 1.91 (dd, J = 14.8, 4.0 Hz, 1 H), 1.70 (dd, J = 14.8, 8.4 Hz, 1 H), 1.35–1.10 (m, 4 H), 1.16 (d, J = 6.4 Hz, 6 H); HRMS (ESI) calcd for $C_{29}H_{36}FN_3O_5$ [(M + H)$^+$], 526.2711; found, 526.2699; Anal. ($C_{29}H_{36}FN_3O_5Na\cdot 1.9H_2O$) C, H, N; HPLC (method B) t_R = 1.93 min (>99%).

(3*R*,5*R*)-7-{2-(4-Fluoro-phenyl)-4-isopropyl-5-[(4-methoxy-benzyl)-methyl-carbamoyl]-2*H*-pyrazol-3-yl}-3,5-dihydroxy-heptanoic Acid Sodium Salt (44). ^{1}H NMR (DMSO-d_6) δ 7.47–7.40 (m, 2 H), 7.13–7.12 (m, 4 H), 6.87–6.81 (m, 2 H), 4.71 (bs, 1 H), 4.54 (s, 1 H), 4.41 (s, 1 H), 3.68–3.66 (m, 3 H), 3.60–3.58 (m, 1 H), 3.45–3.41 (m, 1 H), 2.89–2.86 (m, 1 H), 2.77–2.76 (m, 1 H), 2.75–2.68 (m, 1 H), 2.58–2.52 (m, 1 H), 1.90 (dd, J = 14.8, 4.0 Hz, 1 H), 1.71 (dd, J = 14.8, 8.2 Hz, 1 H), 1.39–1.19 (m, 4 H), 1.14 (d, J = 6.8 Hz, 6 H); HRMS (ESI) calcd for $C_{29}H_{36}FN_3O_5$ [(M + H)$^+$], 542.2660; found, 542.2586; HPLC (method C) t_R = 3.45 min (98.5%).

(3*R*,5*R*)-7-[5-[(2-Fluoro-benzyl)-methyl-carbamoyl]-2-(4-fluoro-phenyl)-4-isopropyl-2*H*-pyrazol-3-yl]-3,5-dihydroxy-heptanoic Acid Sodium Salt (45). ^{1}H NMR (DMSO-d_6) δ 7.55–7.10 (m, 8 H), 4.74 (bs, 1 H), 4.70 (s, 1 H), 4.67 (s, 1 H), 3.65–3.61 (m, 1 H), 3.49–3.45 (m, 1 H), 2.92–2.91 (m, 4 H), 2.88–2.82 (m 1 H), 2.59–2.54 (m, 1 H), 1.92 (dd, J = 14.8, 4.0 Hz, 1 H), 1.71 (dd, J = 14.8, 8.2 Hz, 1 H), 1.42–1.21 (m, 3 H), 1.17–1.11 (m, 6 H); HRMS (ESI) calcd for $C_{28}H_{33}F_2N_3O_5$ [(M + H)$^+$], 530.2461; found, 530.2450; Anal. ($C_{28}H_{33}F_2N_3O_5Na\cdot 1.8H_2O$) C, H, N; HPLC (method A) t_R = 7.01 min (98.0%).

(3*R*,5*R*)-7-[5-[(3-Fluoro-benzyl)-methyl-carbamoyl]-2-(4-fluoro-phenyl)-4-isopropyl-2*H*-pyrazol-3-yl]-3,5-dihydroxy-heptanoic Acid Sodium Salt (46). ^{1}H NMR (DMSO-d_6) δ 7.55–7.10 (m, 8 H), 4.73 (bs, 1 H), 4.66 (s, 1 H), 4.55 (s, 1 H), 3.62–3.59 (m, 1 H), 3.48–3.45 (m, 1 H), 2.94–2.91 (m, 1 H), 2.88–2.82 (m 1 H), 2.86 (s, 3 H), 2.57–2.53 (m, 1 H), 1.91 (dd, J = 14.8, 4.0 Hz, 1 H), 1.72 (dd, J = 14.8, 8.0 Hz, 1 H), 1.43–1.15 (m, 4 H), 1.17 (d, J = 6.8 Hz, 6 H); HRMS (ESI) calcd for $C_{28}H_{33}F_2N_3O_5$ [(M + H)$^+$], 530.2461; found, 530.2448; HPLC (method A) t_R = 7.06 min (96.2%).

(3*R*,5*R*)-7-[5-[(4-Fluoro-benzyl)-methyl-carbamoyl]-2-(4-fluoro-phenyl)-4-isopropyl-2*H*-pyrazol-3-yl]-3,5-dihydroxy-heptanoic Acid Sodium Salt (47). ^{1}H NMR (DMSO-d_6) δ 7.52–7.08 (m, 8 H), 4.71 (bs, 1 H), 4.60 (s, 1 H), 4.48 (s, 1 H), 3.61–3.58 (m, 1 H), 3.47–3.45 (m, 1 H), 2.89–2.86 (m, 1 H), 2.80 (s, 3 H), 2.70–2.61(m, 1 H), 2.57–2.54 (m, 1 H), 1.89 (dd, J = 14.8, 4.0 Hz, 1 H), 1.69 (dd, J = 14.8, 8.2 Hz, 1 H), 1.42–1.10 (m, 4 H), 1.16–1.11 (m, 6

H); HRMS (ESI) calcd for $C_{28}H_{33}F_2N_3O_5$ [$(M + H)^+$], 530.2461; found, 530.2452; HPLC (method B) $t_R = 1.57$ min (99.0%).

(3*R*,5*R*)-7-[5-[(2,4-Difluoro-benzyl)-methyl-carbamoyl]-2-(4-fluoro-phenyl)-4-isopropyl-2*H*-pyrazol-3-yl]-3,5-dihydroxy-heptanoic Acid Sodium Salt (48). ^{1}H NMR (DMSO-d_6) δ 7.53–7.00 (m, 7 H), 4.71 (bs, 1 H), 4.63 (s, 1 H), 4.60 (s, 1 H), 3.61–3.58 (m, 1 H), 3.47–3.42 (m, 1 H), 2.87–2.84 (m, 4 H), 2.78–2.75 (m, 1 H), 2.69–2.65 (m, 1 H), 1.89 (dd, $J = 14.8$, 4.0 Hz, 1 H), 1.71 (dd, $J = 14.8$, 8.2 Hz, 1 H), 1.36–1.11 (m, 4 H), 1.13–1.09 (m, 6 H); HRMS (ESI) calcd for $C_{28}H_{32}F_3N_3O_5$ [$(M + H)^+$], 548.2366; found, 548.2355; HPLC (method A) $t_R = 7.37$ min (>99%).

(3*R*,5*R*)-7-[5-[(2,3-Difluoro-benzyl)-methyl-carbamoyl]-2-(4-fluoro-phenyl)-4-isopropyl-2*H*-pyrazol-3-yl]-3,5-dihydroxy-heptanoic Acid Sodium Salt (49). ^{1}H NMR (DMSO-d_6) δ 7.48–7.02 (m, 7 H), 4.71–4.69 (m, 3 H), 3.59–3.57 (m, 1 H), 3.45–3.43 (m, 1 H), 2.91–2.84 (m, 4 H), 2.72–2.68 (m, 1 H), 2.58–2.53 (m, 1 H), 1.90 (dd, $J = 14.8$, 4.0 Hz, 1 H), 1.69 (dd, $J = 14.8$, 8.0 Hz, 1 H), 1.40–1.08 (m, 4 H), 1.14–1.09 (m, 6 H); HRMS (ESI) calcd for $C_{28}H_{32}F_3N_3O_5$ [$(M + H)^+$], 548.2366; found, 548.2352; Anal. ($C_{27}H_{30}F_3N_3O_5Na$) C, H, N; HPLC (method A) $t_R = 7.33$ min (98.6%).

(3*R*,5*R*)-7-{2-(4-Fluoro-phenyl)-4-isopropyl-5-[*N*-methyl-(*R*)-α-methyl-benzylcarbamoyl]-2*H*-pyrazol-3-yl}-3,5-dihydroxy-heptanoic Acid Sodium Salt (50). ^{1}H NMR (DMSO-d_6) δ 7.46–7.41 (m, 2 H), 7.35–7.10 (m, 7 H), 5.91 (t, $J = 6.8$ Hz, 0.6 H), 5.29 (t, $J = 6.8$ Hz, 0.4 H), 4.70 (bs, 1 H), 3.62–3.60 (m, 1 H), 3.45–3.42 (m, 1 H), 2.90–2.83 (m, 1 H), 2.73–2.69 (m, 1 H), 2.56–2.45 (m, 4 H), 1.93 (dd, $J = 14.8$, 3.6 Hz, 1 H), 1.72 (dd, $J = 14.8$, 8.4 Hz, 1 H), 1.47 (t, $J = 6.8$ Hz, 3 H), 1.41–1.05 (m, 10 H); HRMS (ESI) calcd for $C_{29}H_{36}FN_3O_5$ [$(M + H)^+$], 526.2711; found, 526.2708; Anal. ($C_{28}H_{33}FN_3O_5Na \cdot 1.6H_2O$) C, H, N; HPLC (method A) $t_R = 7.33$ min (97.4%).

(3*R*,5*R*)-7-{2-(4-Fluoro-phenyl)-4-isopropyl-5-[*N*-methyl-(*S*)-α-methyl-benzylcarbamoyl]-2*H*-pyrazol-3-yl}-3,5-dihydroxy-heptanoic Acid Sodium Salt (51). ^{1}H NMR (DMSO-d_6) δ 7.46–7.42 (m, 2 H), 7.35–7.12 (m, 7 H), 5.94 (t, $J = 6.4$ Hz, 0.5 H), 5.24 (t, $J = 6.8$ Hz, 0.5 H), 3.62–3.58 (m, 1 H), 3.45–3.34 (m, 1 H), 2.92–2.85 (m, 1 H), 2.71–2.65 (m, 1 H), 2.59–2.45 (m, 4 H), 1.90 (dd, $J = 14.8$, 4.0 Hz, 1 H), 1.71 (dd, $J = 14.8$, 8.2 Hz, 1 H), 1.47 (t, $J = 7.2$ Hz, 3 H), 1.35–1.05 (m, 10 H); HRMS (ESI) calcd for $C_{29}H_{36}FN_3O_5$ [$(M + H)^+$], 526.2711; found 526.2700; HPLC (method B) $t_R = 1.73$ min (>99%).

(3*R*,5*R*)-7-[2-(4-Fluoro-phenyl)-4-isopropyl-5-(2-phenyl-pyrrolidine-1-carbonyl)-2*H*-pyrazol-3-yl]-3,5-dihydroxy-heptanoic Acid Sodium Salt (52). ^{1}H NMR (DMSO-d_6) [mixture of diastereomers] δ 7.51–7.47 (m), 7.33–7.06 (m), 6.93–6.92 (m), 5.37–5.32 (m), 5.14–5.11 (m), 3.79–3.28 (m), 2.96–2.89 (m), 2.78–2.19 (m), 1.92–1.56 (m), 1.24–0.87 (m); HRMS (ESI) calcd for $C_{30}H_{36}FN_3O_5$ [$(M + H)^+$], 538.2711; found, 538.2700; HPLC (method A) $t_R = 7.01$ min (>99%).

(3*R*,5*R*)-7-[2-(4-Fluoro-phenyl)-4-isopropyl-5-(2-phenyl-piperidine-1-carbonyl)-2*H*-pyrazol-3-yl]-3,5-dihydroxy-heptanoic Acid Sodium Salt (54). ^{1}H NMR (DMSO-d_6) [mixture of diastereomers] δ 7.59–7.50 (m), 7.32–7.23 (m) 5.91–5.89 (m), 4.74–4.72 (m), 3.65–3.61 (m), 3.35–3.32 (m), 2.91–2.47 (m), 1.94–1.90 (m) 1.85–1.62 (m), 1.59–1.10 (m); HRMS (ESI) calcd for $C_{31}H_{38}FN_3O_5$ [$(M + H)^+$], 552.2868; found, 552.2854; HPLC (method A) $t_R = 7.75$ min (95.9%).

(3*R*,5*R*)-7-[2-(4-Fluoro-phenyl)-4-isopropyl-5-(3-phenyl-piperidine-1-carbonyl)-2*H*-pyrazol-3-yl]-3,5-dihydroxy-heptanoic Acid Sodium Salt (55). ^{1}H NMR (DMSO-d_6) δ 7.54–7.48 (m, 2 H), 7.24 (t, $J = 4.8$ Hz, 1 H), 7.39–7.11 (m, 6 H), 4.73 (d, $J = 7.6$ Hz, 1 H), 3.62 (dd, $J = 18.0$, 4.0 Hz, 1 H), 3.79–3.68 (m, 2 H), 3.61–3.58 (m, 1 H), 3.25–3.23 (m, 1 H), 3.05–2.99 (m, 1 H), 2.91–2.79 (m, 1 H), 2.78–2.52 (m, 3 H), 1.98–1.85 (m, 2 H), 1.84–1.61 (m, 3 H), 1.55–1.10 (m, 10 H); HRMS (ESI) calcd for $C_{31}H_{38}FN_3O_5$ [$(M + H)^+$], 552.2868; found, 552.2851; HPLC (method A) $t_R = 7.74$ min (98.0%).

Isolation of Rat Liver Microsomes. Male Charles River Sprague–Dawley rats were fed with 2.5% cholestyramine in rat chow diets for 7 days before sacrificing. Livers were minced and homogenized in a sucrose homogenizing solution in an ice bath. Homogenates were diluted into a final volume of 200 mL and centrifuged for 0.25 h with a Sorvall centrifuge at 5 °C, 10000 rpm (12000× G). The upper fat layer was removed and the supernatant was decanted into fresh tubes. This step was repeated twice prior to transferring the supernatant into ultracentrifuge tubes, which were centrifuged at 36000 rpm (105000× G) for 1 h at 5 °C. The resulting supernatant was discarded and the pellet was added to a total of 15 mL of 0.1 M KH_2PO_4. Pellets were then homogenized gently by hand. Samples were pooled and diluted into a total of 60 mL buffer. The protein concentration of the homogenate was determined by the Lowry method using a BCA (bicinchoninic acid) kit from Pierce Chemical Company. Aliquots (1 mL) of microsomes were subsequently kept frozen in liquid nitrogen.

HMG-CoA Reductase Assay Procedure. DMSO (1 μL) or DMSO (1 μL) containing a test compound at a concentration of between 0.1 to 1 nM was placed into each well of a Corning 96 well plate. A volume of 34 μL buffer [100 mM NaH_2PO_4, 10 mM imidazole and 10 mM EDTA (ethylenediamine−tetraacetic acid)] containing 35 μg/mL rat liver microsomes was added into each well. After incubation for 0.5 h on ice, 15 μL of ^{14}C-HMGCoA (0.024 μCi) with 15 mM NADPH, 25 mM DTT, (dithiothreitol) was added and incubated at 37 °C for an additional 0.75 h. The reaction was terminated by the addition of 10 μL of 2 M HCl, followed by the addition of 5 μL of 0.10 M mevalonolactone. Plates were incubated at room temperature for 1 h to allow lactonization of mevalonate to mevalonolactone. The incubated samples were applied to columns containing 300 μL of AGI-X8 anion exchange resin in a Corning filter plate. The eluates were collected into Corning 96 well capture plates. Scintillation cocktail (Ultima-Flo-M) was added into each well and plates counted on a Trilux Microbeta Counter. The IC_{50} values were calculated with GraphPad software (Prism).

Procedure for Sterol Biosynthesis Assay in Rat Hepatocytes. Frozen rat hepatocyctes purchased from Xeno Tech were seeded on a six-well collagen 1 coated plates at a density of 105 cells/well. The cells were grown in DMEM (Dulbecco's modified Eagle medium, Gibco, 11054-020) containing 10% FBS (fetal bovine serum) and 10 mM HEPES (*N*-2-hydroxyethyl-piperazie-N^1-2-ethane sulfonic acid, Gibco 15630-080) for 24 h. The cells were preincubated with compounds for 4 h and then labeled by incubating in medium containing 1 μCi/mL of ^{14}C acetic acid for an additional 4 h. After labeling, the cells were washed twice with 5 nM MOPS (3-[*N*-morpholino]propane sulfonic acid) solution containing 150 mM NaCl and 1 nM EDTA and collected in the lysis buffer containing 10% KOH and 80% ethanol. To separate labeled cholesterol from labeled noncholesterol lipids, the cells lysates were subject to saponification at 60 °C for 2 h. The lysates were then combined with 0.5 volume of H_2O and 2 volumes of hexane, followed by 0.5 h of vigorous shaking. After the separation of two phases, the upper-phase solution was collected and combined with 5 volumes of scintillation cocktail. The amount of ^{14}C cholesterol was quantified by liquid scintillation counting. The IC_{50} values were calculated with GraphPad software (Prism 3.03).

Procedure for Sterol Biosynthesis L6 Rat Myoblasts. L6 rat myoblasts purchased from ATCC (CRL-1458) were grown in T-150 vented culture flasks and seeded on 12-well culture plates at a density of 60000 cells per well. The cells were grown in DMEM containing 10% heat inactivated FBS for 72 h until reaching confluence. The cells were preincubated in media with compound and 0.20% DMSO for 3 h and then labeled by incubating in medium containing compound, 0.20% DMSO and 1 μCi/mL of ^{14}C acetic acid for an additional 3 h. After labeling, the cells were washed once with PBS then lysed overnight at 4 °C in buffer containing 10% KOH and 78% ethanol. Lipid ester bonds were hydrolyzed by saponification of the lysates at 60 °C for 2 h. Sterols (including cholesterol) were extracted from saponified lysates by combining with 3 volumes of hexane and mixing by pipet six times. The upper organic phase solution was collected and combined with an equal volume of 1 N KOH in 50% methanol and mixed by pipet six times.

The upper organic phase was collected in a scintilant-coated plate, and hexanes were removed by evaporation at room temperature for 3 h. The amount of ^{14}C cholesterol was quantified by scintillation counting in a Triflux 1450 plate reader (Wallac). The IC_{50} values were calculated from % inhibitions relative to negative controls versus compound concentration on Microsoft excel 2000 data analysis wizard using a sigmoid inhibition curve model with the following formula: $y = B_{max}(1 - (X^n/K^n + X^n)) + Y2$, where K is the IC_{50} for the inhibition curve, X is inhibitor concentration, Y is the response being inhibited, and $B_{max} + Y2$ is the limiting response as X approaches zero.

Hamster Acute In Vivo Study Protocol..[28] Male Golden Syrian Hamsters were acquired from Charles River for use in these studies. Upon delivery, the hamsters were randomly divided into treatment and control groups of eight animals each and acclimated to a reverse light cycle for 5–11 days. While acclimating to the reverse light cycle, the hamsters were allowed to consume ad libitum normal rodent chow (Research Diets, Purina 5001). Three days prior to the date of the study, the hamsters were transferred to wire-bottom flush caging, and the normal rodent chow was replaced by normal rodent chow with the addition of 2.5% cholestyramine. Hamsters were allowed access to food and water throughout the study period.

Each group ($n = 8$) of hamsters were dosed with either vehicle or vehicle plus test compound via oral gavage at a volume equivalent to 0.25% body weight. Either 2 ($t = 2$–4 h assay) or 4 h ($t = 4$– 6h assay) postdose, each animal was injected (i.p.) with 80 μCi of ^{14}C sodium acetate (Amersham Biosciences, CFQ30013) in 1 mL of 0.9% NaCl. At 4 ($t = 2$–4 h assay) or 6 h ($t = 4$–6 h assay) postdose, the hamsters were euthanized via CO_2, followed by blood collection via cardiac stick. Each sample of blood collected was centrifuged for 10 min at 3000 RPM at 5 °C. After separation, 400 μL of plasma were removed from each tube and placed in a 16 × 100 M culture tube for future saponification and extraction of cholesterol esters.

To each 400 μL sample of plasma were added 500 μL of saline, 100 μL of ^{3}H cholesterol (internal standard for extraction), and 2.5 mL of 10% KOH. After vortexing, the rack of sample tubes was placed in a water bath preheated to 75 °C for one hour to complete the saponification process. The sample rack was removed from the water bath after one hour and allowed to cool for approximately 15 min. At this point, 2.5 mL of petroleum ether was added to extract the cholesterol esters. The rack was placed on a shaker, and the solutions were mixed for 10 min. The tubes were then centrifuged for 10 min at 3000 RPM and 5 °C to separate the organic and aqueous phases. Using a 2500 μL pipettor and proceeding in groups, 1.2 mL of the organic supernatant was drawn from each culture tube and expressed into a correspondingly numbered 7 mL scintillation vial. Each vial had 5.1 mL of scintillation fluid added to it and was capped for further analysis. Included in the sample analysis were three 7 mL scintillation vials containing 6.3 mL of scintillation fluid serving as blanks, three 7 mL scintillation vials containing 100 μL of ^{3}H cholesterol added to 6.3 mL of scintillation fluid to provide the denominator in the calculation of the percent extraction of the internal standard, and 2 μL of the 80 μCi of ^{14}C sodium acetate/0.9% NaCl solution in 6.3 mL of scintillation fluid to measure consistency of count between aliquots.

Seven-Day Guinea Pig LDL-Lowering Assay. Male Hartley guinea pigs (300–500 g initial body weight) were obtained from Charles River, pair housed in guinea pig caging under a 12 h light and dark cycle, and given Guinea Pig Laboratory Diet 5025 and water ad libitum. Animals were allowed to acclimate in house for at least 1 week prior to the study. During the experiment, the animals were fed guinea pig chow (Laboratory diet 5025). Prior to the start of dosing, animals were identified using implantable chips (Bio Medic Data Inc., model IMI-1000). Body weights were obtained at the start of each week to calculate daily doses. Animals were randomly assigned to vehicle ($n = 8$) or drug treatment ($n = 8$) groups. All compound suspensions were administered (5 mL/kg) starting on day one and were dosed daily through day 8 via oral gavage. On day 8, animals were dosed and then sacrificed using CO_2 approximately 2 h postdose. Blood was collected in EDTA anticoagulant for analysis of plasma drug levels, total cholesterol, triglycerides, and lipid profile.

Acknowledgment. We would like to acknowledge the technical contributions made by Fang Sun, Loola Al-Kassim, Susan Holly, Cindy Spessard, and Siradanahalli Guru. We would also like to thank Barry Finzel for his assistance with the X-ray structure of compound **50**.

Supporting Information Available: Elemental analysis or HRMS and HPLC purity data for final compounds **2**, **3**, **32**–**52**, and **54**, and **55**. This material is available free of charge via the Internet at http://pubs.acs.org.

References

(1) Grundy, S. M. Primary prevention of coronary heart disease: Role of cholesterol control in the United States. *J. Intern. Med.* **1997**, *241*, 295–306.

(2) (a) Verschuren, W. M.; Jacobs, D. R.; Bloemberg, B. P.; Kromhout, D.; Menotti, C.; Aravanis, H.; Blackburn, R.; Buzina, A. S.; Dontas, F.; Fidanza, F. Serum total cholesterol and long-term coronary heart disease mortality in different cultures. Twenty-five-year follow-up of the seven countries study. *JAMA, J. Am. Med. Assoc.* **1995**, *274*, 131–136. (b) Manninen, V.; Tenkanen, L.; Koskinen, P; Huttunen, J. K.; Manttari, M.; Heinonen, O. P.; Frick, M. H. Joint effects of serum triglyceride and LDL cholesterol and HDL cholesterol concentrations on coronary heart disease risk in the Helsinki Heart Study; Implication for treatment. *Circulation* **1992**, *85*, 37–45. (c) Wilson, P. W.; Kannel, W. B.; Silbershatz, H.; D'Agostino, R. B. Clustering of metabolic factors and coronary heart disease. *Arch. Intern. Med.* **1999**, *159*, 1104–1109.

(3) (a) For reviews, see: McKenney, J. M. Pharmacologic characteristics of statins. *Clin. Cardiol. (Suppl. III).* **2003**, *26*, 32–38. (b) Speidal, K. M.; Hilleman, D. E. Pharmacoeconomic considerations with statin therapy. *Expert Opin. Pharmacother.* **2006**, *7*, 1291–1304.

(4) (a) Scandinavian Simvastatin Survival Study Investigators. Randomized trial of cholesterol lowering in 4444 patients with coronary heart disease: the Scandinavian Simvastatin Survival Study (4S). *Lancet*, **1994**, *344*, 1383–1389; (b) The Long-Term Intervention with Pravastatin in Ischemic Disease (LIPID) Study Group Prevention of cardiovascular events and death with pravastatin in patients with coronary heart disease and a broad range of initial cholesterol levels. *N. Engl. J. Med.* **1998**, *339*, 1349–1357; (c) Shepard, J.; Cobbe, S. M.; Ford, I.; Isles, C. G.; Lorimer, A. R.; MacFarlane, P. W.; McKillop, J. H.; Pachard, C. J. Prevention of coronary heart disease with pravastatin in men with hypercholesterolemia. *N. Engl. J. Med.* **1995**, *333*, 1301–1307. (d) LaRosa, J. C.; He, J.; Vupputuri, S. Effects of statins on risk of coronary disease. *JAMA, J. Am. Med. Assoc.* **1999**, *282*, 2340–2346.

(5) (a) LaRosa, J. C.; Grundy, S. M.; Walters, D. D.; Shear, C.; Barter, P.; Fruchart, J.-C.; Gotto, A. M.; Greten, H.; Kastelein, J. J. P.; Shepard, J.; Wenger, N. K. Intensive lipid lowering with atorvastatin in patients with stable coronary disease. *N. Engl. J. Med.* **2005**, *352*, 1425–1435. (b) Schwartz, G.; Olsson, A. G.; Ezekowitz, M. D.; Ganz, P.; Oliver, M. F.; Waters, D.; Zeiher, A.; Chaitman, B. R.; Leslie, S.; Stern, T. Effects of atorvastatin on early recurrent ischemic events in acute coronary syndromes. *JAMA, J. Am. Med. Assoc.* **2001**, *285*, 17111718. (c) Cannon, C. P.; Braunwald, E.; McCabe, C. H.; Rader, D. J.; Rouleau, J. L.; Belder, R.; Joyal, S. V.; Hill, K.; Pfeffer, M. A.; Skene, A. M. Intensive versus moderate lipid lowering with statins after acute coronary syndromes. *N. Engl. J. Med.* **2004**, *350*, 1495–1504. (d) Cannon, C. P.; Steinberg, B. A.; Murphy, S. A.; Mega, J. L.; Braunwald, E. Meta-analysis of cardiovascular outcome trials comparing intensive versus moderate statin therapy. *J. Am. Coll. Cardiol.* **2006**, *48*, 438–445.

(6) Grundy, S. M.; Cleeman, J. I.; Merz, N. B.; Brewer, B.; Clark, L. T.; Hunninghake, D. B.; Pasternak, R. C.; Smith, S. C.; Stone, N. J. Implications of recent clinical trials for the National Cholesterol Education Adult Treatment Panel III guidelines. *Circulation* **2004**, *110*, 227–239.

(7) O'Keefe, J. H.; Cordain, L.; Harris, W. H.; Moe, R. M.; Vogel, R. Optimal low-density lipoprotein is 50 to 70 mg/dl. *J. Am. Coll. Cardiol.* **2004**, *43*, 2142–2146.

(8) For a review, see: Patel, T. N.; Shishehbor, M. H.; Bhatt, D. L. A review of high dose statin therapy: Targeting cholesterol and inflammation in atherosclerosis. *Eur. Heart J.* **2007**, *28*, 664–672.

(9) (a) Brukert, E.; Hayem, G.; Dejager, S.; Yau, C.; Begaud, B. Mild to moderate muscular symptoms with high-dosage statin therapy in hyperlipidemic patients–The PRIMO study. *Cardiovasc. Drugs Ther.*

2005, *19*, 403–414. (b) Baer, A. N.; Wortmann, R. L. Myotoxicity associated with lipid-lowering drugs. *Curr. Opin. Rheumatol.* **2007**, *19*, 67–73. (c) Tiwari, A.; Bansal, V.; Chugh, A.; Mookhtiar, K. Statins and myotoxicity: a therapeutic limitation. *Expert Opin. Drug Saf.* **2006**, *5*, 651–666. (d) Athar, H.; Shah, A. R.; Thompson, P. D. Possible mechanisms for statin myopathy and its relationship to physical exercise. *Future Lipidol.* **2006**, *1*, 143–151. (e) Franc, S.; Dejager, S.; Bruckert, E.; Chauvenet, M.; Giral, P.; Turpin, G. A comprehensive description of muscle symptoms associated with lipid-lowering drugs. *Cardiovasc. Drugs Ther.* **2003**, *17*, 459–465.

(10) (a) For reviews, see: Hamelin, B. A.; Turgeon, J. Hydrophilicity/lipophilicity: Relevance for the pharmacology and clinical effects of HMG-CoA reductase inhibitors. *Trends Pharmacol. Sci.* **1998**, *19*, 26–37. (b) Rosenson, R. S.; Tangney, C. C. Antiatherothrombotic properties of statins. *JAMA, J. Am. Med. Assoc.* **1998**, *279*, 1643–1650. See also: (c) Schachter, M. Chemical, pharmacokinetic, and pharmacodynamic properties of statins: an update. *Fundam. Clin. Pharmacol.* **2004**, *19*, 117–125. (d) Ho, R. H.; Tirona, R. G.; Leake, B. F.; Glaeser, H.; Lee, W.; Lemke, C. J.; Wang, Y.; Kim, R. B. Drug and bile acid transporters in rosuvastatin hepatic uptake: Function, expression, and pharmacogenetics. *Gastroenterology* **2006**, *130*, 1793–1806.

(11) (a) Roth, B. D.; Bocan, T. M.; Blankey, C. J.; Chucholowski, A. W.; Creger, P. L.; Creswell, M. W.; Ferguson, E.; Newton, R. S.; O'Brien, P.; Picard, J. A.; Roark, W. H.; Sekerke, C. S.; Sliskovic, D. R.; Wilson, M. W. Relationship between tissue selectivity and lipophilicity for inhibitors of HMG-CoA reductase. *J. Med. Chem.* **1991**, *34*, 463–466. (b) Koga, T.; Shimada, Y.; Kuroda, M.; Tsujita, Y.; Hasegawa, K.; Yamazaki, M. Tissue-selective inhibition of cholesterol synthesis in vivo by pravastatin sodium, a 3-hydroxy-3-methylglutaryl coenzyme A reductase inhibitor. *Biochim. Biophys. Acta* **1990**, *1045*, 115–120. (c) Balasubramanian, N.; Brown, P. J.; Catt, J. D.; Han, W. T.; Parker, R. A.; Sit, S. Y.; Wright, J. J. A potent, tissue-selective, synthetic inhibitor of HMG-CoA reductase. *J. Med. Chem.* **1989**, *32*, 2038–2041. (d) Joshi, H. N.; Fakes, M. G.; Serajuddin, A. M. Differentiation of 3-hydroxy-3-methylgltaryl-coenzyme A reductase inhibitors by their relative lipophilicity. *Pharm. Pharmacol. Commun.* **1999**, *5*, 269–271.

(12) (a) For a similar study utilizing hepatocyte and endothelial cells, see: van Vliet, A. K.; van Thiel, G. C. F.; Huisman, R. H.; Moshage, H.; Yap, S. H.; Cohen, L. H. Different effects of 3-hydroxy-3-methylglutaryl-coenzyme A reductase inhibitors on sterol synthesis in various human cell types. *Biochim. Biophys. Acta* **1995**, *1254*, 105–111. (b) Corsini, A.; Raiteri, M.; Soma, M.; Fumagalli, R.; Paoletti, R. Simvastatin but not pravastatin inhibits the proliferation of rat aorta myocytes. *Pharmacol. Res.* **1991**, *23*, 173–180.

(13) Hsiang, B.; Zhu, Y.; Wang, Z.; Wu, Y.; Sasseville, V.; Yang, W.-P.; Kirchgessner, T. G. A novel human hepatic organic anion transporting polypeptide (OATP2). *J. Biol. Chem.* **1999**, *274*, 37161–37168.

(14) Ziegler, K.; Hummelsiep, S. Hepatoselective carrier-mediated sodium-independent uptake of pravastatin and pravastatin-lactone. *Biochim. Biophys. Acta* **1993**, *1153*, 23–33.

(15) Nezasa, K.; Higaki, K.; Takeuchi, M.; Nakano, M.; Koike, M. Uptake of rosuvastatin by isolated rat hepatocyctes: comparison with pravastatin. *Xenobiotica* **2003**, *33*, 379–388.

(16) (a) For further discussion of other heterocyclic cores, see: Pfefferkorn, J. A.; Song, Y.; Sun, K.-L.; Miller, S. R.; Trivedi, B. K.; Choi, C.; Sorenson, R.; Bratton, L. D.; Unangst, P. C.; Larsen, S. D.; Askew, V.; Dillon, L.; Hanselman, J. C.; Lin, Z.; Lu, G.; Robertson, A.; Olsen, K.; Mertz, T.; Sekerke, C.; Auerbach, B.; Pavlovsky, A.; Harris, M. S.; Bainbridge, G.; Caspers, N.; Chen, H.; Eberstadt, M. Design and synthesis of hepatoselective, pyrrole-based HMG-CoA reductase inhibitors. *Bioorg. Med. Chem. Lett.* **2007**, *17*, 4538–4544. (b) Pfefferkorn, J. A.; Choi, C.; Song, Y.; Trivedi, B. K.; Larsen, S. D.; Askew, V.; Dillon, L.; Hanselman, J. C.; Lin, Z.; Lu, G.; Robertson, A.; Sekerke, C.; Auerbach, B.; Pavlovsky, A.; Harris, M. S.; Bainbridge, G.; Caspers, N. Design and synthesis of novel, conformationally restricted HMG-CoA reductase inhibitors. *Bioorg. Med. Chem. Lett.* **2007**, *17*, 4531–4537.

(17) Broggini, G.; Casalone, G.; Garanti, L.; Molteni, G.; Pilati, T.; Zecchi, G. Asymmetric induction by the (*S*)-1-phenylethyl group in intramolecular nitrile imine cycloadditions giving enantiopure 3,3*a*-dihydropyrazolo[1,5-*a*][1,4]benzodiazepine-4(6*H*)-ones. *Tetrahedron: Asymmetry* **1999**, *10*, 4447–4554.

(18) Buttero, P. D.; Molteni, G.; Pilati, T. Nitrilimine cycloaddition to 4-(pyrazol-5-yl)carbonyl-2-azetidinone and 4-(pyrazol-4-yl)carbonyl-2-azetidinone. *Tetrahedron Lett.* **2003**, *44*, 1425–1427.

(19) Ghosh, D.; Snyder, S. E.; Watts, V. J.; Mailman, R. B.; Nichols, D. E. 8,9-Dihydroxy-2,3,7,11b-tetrahydro-1*H*-naph[1,2,3-de]isoquinoline: A potent full dopamine D_1 agonist containing a rigid β-phenyldopamine pharmacophore. *J. Med. Chem.* **1996**, *39*, 549–555.

(20) For the discussion of a related synthesis, see: Pfefferkorn, J. A.; Bowles, D. M.; Kissel, W.; Bolyles, D. C.; Choi, C.; Larsen, S. D.; Song, Y.; Sun, K.-L.; Miller, S.; Trivedi, B. K. Development of a practical synthesis of novel, pyrrole-based HMG-CoA reductase inhibitors. *Tetrahedron* **2007**, *63*, 8124–8134.

(21) Radl, S. A new way to *tert*-butyl [(4*R*,6*R*)-6-aminoethyl-2,2-dimethyl-1,3-dioxan-4-yl]acetate, a key intermediate of atorvastatin synthesis. *Synth. Commun.* **2003**, *33*, 2275–2283.

(22) Konoike, T.; Araki, Y. Practical synthesis of chiral synthons for the preparation of HMG-CoA reductase inhibitors. *J. Org. Chem.* **1994**, *59*, 7849–7854.

(23) Chen, K.-M.; Hardtmann, G. E.; Prasad, K.; Repic, O.; Shapiro, M. J. 1,3-*syn* diastereoselective reduction of β-hydroxyketones utilizing alkoxydialkylboranes. *Tetrahedron Lett.* **1987**, *28*, 155–158.

(24) Coordinates for the X-ray structure of Figure 2 have been deposited at the PDB under the file name 2R4F. For crystallization conditions, see ref 16a.

(25) For a review, see: Istvan, E. Statin inhibition of HMG-CoA reductase: A 3-dimensional view. *Atherosclerosis Suppl.* **2003**, *4*, 3–8.

(26) This selection criteria HMG-CoA $IC_{50} = 1$–10 nM resulted only in the exclusion of compound **38**. The criteria was implemented to minimize the potentially confounding effect of inherent analog potency on the analysis.

(27) (a) For a discussion of lipophilicity and membrane permeability, see: Chou, C.-H.; McLachlan, A. J.; Rowland, M. Membrane permeability and lipophilicity in the isolated perfused rat liver: 5-ethyl barbituric acid and other compounds. *J. Pharmacol. Exp. Ther.* **1995**, *275*, 933–940. (b) van de Waterbeemd, H.; Camenisch, G.; Folkers, G.; Raevsky, O. A. Estimation of caco-2 cell permeability using calculated molecular descriptors. *Quant. Struct.-Act. Relat.* **1996**, *15*, 480–490. (c) Bermejo, M.; Avdeef, A.; Ruiz, A.; Nalda, R.; Ruell, J. A.; Tsinman, O.; Gonzalez, I.; Fernandez, C.; Sanchez, G.; Garrigues, T. M.; Merino, V. PAMPA—A drug absorption in vitro model 7. Comparing rat in situ, caco-2, and PAMPA permeability of fluoroquinolones. *Eur. J. Pharm. Sci.* **2004**, *21*, 429–441.

(28) For a related assay, see: Aoki, T.; Nisimura, H.; Nakagawa, S.; Kojima, J.; Suzuki, H.; Tamaki, T.; Wada, Y.; Yokoo, N.; Sato, F.; Kimata, H.; Kitahara, M.; Toyoda, K.; Sakashita, M.; Saito, Y. Pharmacological profile of a novel synthetic inhibitor of 3-hydroxy-3-methylglutaryl-coenzyme A reductase. *Arzneim.-Forsch. Drug Res.* **1997**, *47*, 904–909.

JM070849R